

Accepted Manuscript

QSAR-driven design, synthesis and discovery of potent chalcone derivatives with antitubercular activity

Marcelo N. Gomes, Rodolpho C. Braga, Edyta M. Grzelak, Bruno J. Neves, Eugene Muratov, Rui Ma, Larry L. Klein, Sanghyun Cho, Guilherme R. Oliveira, Scott G. Franzblau, Carolina Horta Andrade

PII: S0223-5234(17)30387-2

DOI: [10.1016/j.ejmech.2017.05.026](https://doi.org/10.1016/j.ejmech.2017.05.026)

Reference: EJMECH 9456

To appear in: *European Journal of Medicinal Chemistry*

Received Date: 9 February 2017

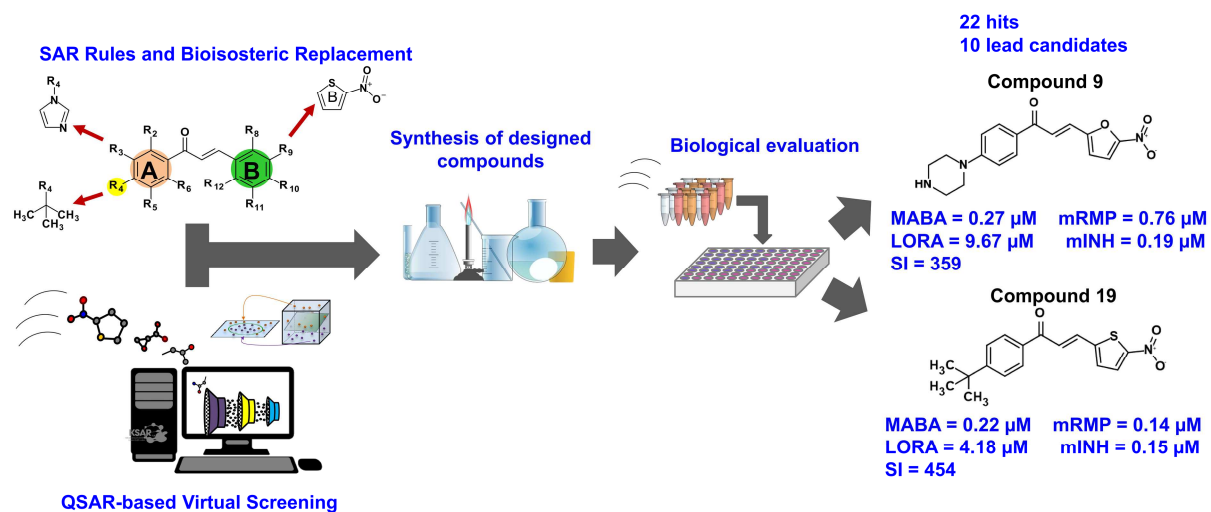
Revised Date: 4 May 2017

Accepted Date: 8 May 2017

Please cite this article as: M.N. Gomes, R.C. Braga, E.M. Grzelak, B.J. Neves, E. Muratov, R. Ma, L.L. Klein, S. Cho, G.R. Oliveira, S.G. Franzblau, C.H. Andrade, QSAR-driven design, synthesis and discovery of potent chalcone derivatives with antitubercular activity, *European Journal of Medicinal Chemistry* (2017), doi: 10.1016/j.ejmech.2017.05.026.

This is a PDF file of an unedited manuscript that has been accepted for publication. As a service to our customers we are providing this early version of the manuscript. The manuscript will undergo copyediting, typesetting, and review of the resulting proof before it is published in its final form. Please note that during the production process errors may be discovered which could affect the content, and all legal disclaimers that apply to the journal pertain.





1 QSAR-driven Design, Synthesis and Discovery 2 of Potent Chalcone Derivatives with 3 Antitubercular Activity

4 *Marcelo N. Gomes,[†] Rodolpho C. Braga,[†] Edyta M. Grzelak,[‡] Bruno J. Neves,^{†‡} Eugene*
5 *Muratov,^{#,£,¥} Rui Ma,[‡] Larry L. Klein,[‡] Sanghyun Cho,[‡] Guilherme R. Oliveira,[§] Scott G.*
6 *Franzblau,^{‡*} Carolina Horta Andrade^{†*}*

7 [†]LabMol – Laboratory for Molecular Modeling and Drug Design, Faculdade de Farmácia,
8 Universidade Federal de Goiás, Rua 240, Qd.87, Setor Leste Universitário, Goiânia, Goiás
9 74605-510, Brazil

10 [‡]Institute for Tuberculosis Research, University of Illinois at Chicago, 833 South Wood
11 Street, Chicago, Illinois 60612, United States

12 ^{†‡}Postgraduate Program of Society, Technology and Environment, University Center of
13 Anápolis/UniEVANGELICA, Anápolis, Goiás, 75083-515, Brazil

14 [#]Laboratory for Molecular Modeling, Eshelman School of Pharmacy, University of North
15 Carolina, Chapel Hill, North Carolina 27955-7568, United States

16 [£] Department of Chemical Technology, Odessa National Polytechnic University, Odessa,
17 65000, Ukraine

18 [§] Chemistry Institute, Universidade Federal de Goiás, Goiania, Brazil

19 [¥] Currently Visiting Professor in Universidade Federal de Goiás, Goiania, Brazil

ACCEPTED MANUSCRIPT

ABSTRACT

New anti-tuberculosis (anti-TB) drugs are urgently needed to battle drug-resistant *Mycobacterium tuberculosis* strains and to shorten the current 6-12-month treatment regimen. In this work, we have continued the efforts to develop chalcone-based anti-TB compounds by using an *in silico* design and QSAR-driven approach. Initially, we developed SAR rules and binary QSAR models using literature data for targeted design of new heteroaryl chalcone compounds with anti-TB activity. Using these models, we prioritized 33 compounds for synthesis and biological evaluation. As a result, 10 heteroaryl chalcone compounds (**4**, **8**, **9**, **11**, **13**, **17-20**, and **23**) were found to exhibit nanomolar activity against replicating mycobacteria, low micromolar activity against nonreplicating bacteria, and nanomolar and micromolar against rifampin (RMP) and isoniazid (INH) monoresistant strains (rRMP and rINH) (<1 μ M and <10 μ M, respectively). The series also show low activity against commensal bacteria and generally show good selectivity toward *M. tuberculosis*, with very low cytotoxicity against Vero cells (SI = 11-545). Our results suggest that our designed heteroaryl chalcone compounds, due to their high potency and selectivity, are promising anti-TB agents.

KEYWORDS: Tuberculosis, *in silico* design, QSAR, nitroaromatic compounds, chalcone, anti-TB agents.

INTRODUCTION

Tuberculosis (TB) is a chronic infectious disease caused predominantly by *Mycobacterium tuberculosis* (*M. tb.*). Tuberculosis is reported in every country around the globe and the World Health Organization (WHO) estimates that about a third of the world's population is infected with *M. tb.* [1–3]. According to the WHO, in 2014 there were registered almost 10 million of new TB cases and 1.5 million deaths; 400,000 of which were HIV-positive. As a frequent co-infection, TB is aggravated by the spread of HIV and is a major cause of death among HIV/AIDS patients [3–5].

Drug-sensitive TB can be cured by a combination of isoniazid (INH), rifampin (RMP), pyrazinamide (PZA), and ethambutol (EMB) taken under supervision for 4 months, and 2 months of treatment with only two drugs RMP and INH, consisting the basis of the DOTS program (*Directly Observed Therapy Short-course*). The emergence of multidrug-resistance (MDR-TB) and extensively drug-resistant (XDR-TB) has created substantial new challenges for TB treatment [6,7]. The treatment of resistant strains requires a prolongation of the therapy with drugs that are more toxic, less effective, and more costly [8]. Over the past 16 years, significant investment by academia, funding agencies, and initiatives such as WHO Stop TB Partnership [9] and The Global Alliance for TB Drug Development [10], has led to a renaissance of research in the field of TB and led to the discovery of bedaquiline and delamanid, two new anti-TB drugs approved in 2012 and 2013 respectively for treatment of adults with MDR-TB [11,12].

The development of computer science has found broad application in the drug discovery area [13]. Computer-aided drug design (CADD) has become an integral part of the drug discovery process in both academia and pharma companies [13,14]. Elucidation of quantitative structure-activity relationships (QSAR) is one of the main approaches of CADD

[15–18]. QSAR modeling has been widely used for identification of novel anti-TB agents. In many studies, QSAR was used to design new anti-TB agents [2,19–32]. However, in most the cases, QSAR has been used to modify previously discovered congeneric series of chemicals (Table S1, supplementary material).

Chalcones or 1,3-diaryl-2-propen-1-ones represent one class of natural products and essential intermediates in the biosynthesis of flavonoids. Chalcones are low molecular weight compounds possessing a broad spectrum of biological activities [33–46] including antibacterial [47,48] and anti-TB [38,49,50] activities.

The goal of this work was the design, synthesis and discovery of new chalcone and heteroaryl chalcones with potent anti-TB activity. To achieve this goal, we performed the following steps: (i) collection of available data and rigorous data curation; (ii) generation of structure-activity relationships (SAR) using matched molecular pair analysis (MMPA) to design new chalcones with potential anti-TB activity by bioisosteric replacement; (iii) development of rigorously validated binary QSAR models; (iv) perform virtual screening of designed compounds; (v), organic synthesis and structure identification (NMR, MS, and IR) of selected VS hits; and (vi) *in vitro* experimental evaluation of designed hits under normoxic (MABA) and hypoxic (LORA) conditions.

RESULTS AND DISCUSSION

Design of chalcone and heteroaryl chalcone compounds

For the initial design of new chalcone derivatives with anti-TB activity, we retrieved 604 chalcones compounds with inhibition data against *M. tb.* H37Rv from PubChem Bioassay [51], ChEMBL [52], SciFinder database [53], and from literature. After collecting and integrating all the data, chemical structures and activity values were rigorously curated

following the protocols established by Fourches et al [54–56]. Briefly, structural normalization of specific chemotypes, such as aromatic and nitro groups, was performed using ChemAxon Standardizer (v. 15.10.12.0, ChemAxon, Budapest, Hungary, <http://www.chemaxon.com>). Inorganic salts, organometallic compounds, and mixtures were also removed. After structural standardization, the duplicates were identified using ISIDA Duplicates[57] and HiT QSAR[58]. Analysis of duplicates also allowed to estimate inter- and intra-lab variability. No suspicious data sources were found.

The curated dataset consisted of 571 chalcones, which were the subject for SAR analysis using matched molecular pairs analysis (MMPA, Figure 1). Matched Molecular Pairs Analysis (MMPA) is a useful approach in drug discovery to identify and compare matched molecular pairs from a set of compounds and determining the property change associated [59]. Matched pairs are molecules that differ only by a particular, well defined, structural transformation and are used to study changes in biological properties [60]. Therefore, the MMPA can reveals changes in biological properties between structures with high similarity. In our work, we used the MACCS keys descriptor [61] and Tanimoto coefficient [62] to evaluate structural similarity related with the changes in biological activity (Figure 1).

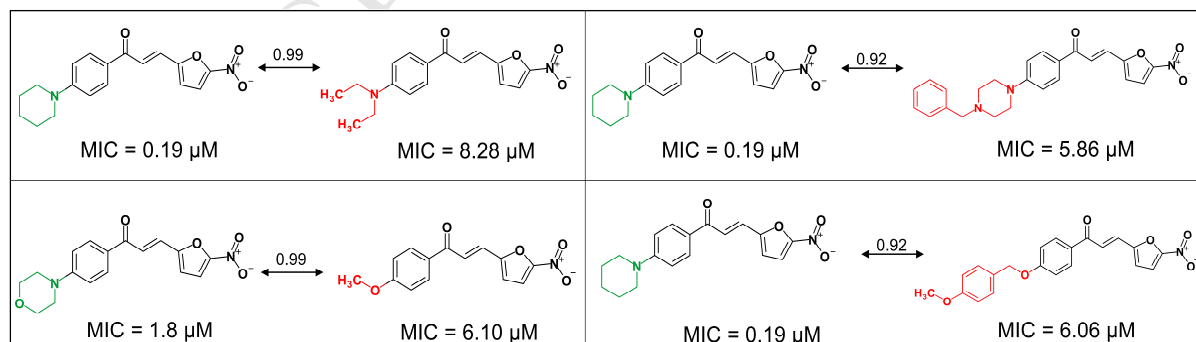


Figure 1. MMPA of selected molecular pairs of chalcones and heteroaryl chalcones with anti-TB activity reported in the literature. The number above the arrows indicate the Tanimoto coefficient between the molecular pair (high structural similarity, Tanimoto

coefficient > 0.90). The groups in green and in red represent the structural differences between the molecules.

The information revealed by the matched molecular pairs allowed us to derive the following SAR rules (Figure 2): (i) hydrophobic and hydrogen bond acceptor groups, e.g., halogens, phenyl, and heterocyclic amines, in *p*-position of ring A are favorable to anti-TB activity; (ii) substitution of benzene ring B by nitrofur, increases the activity; (iii) any substituent in any position of ring B decreases the activity; and (iv) halogen in *ortho*- or *meta*-position of the ring A decreases the activity. These SAR rules were used to design new compounds using the bioisosteric replacement in the BROOD v.2.0 software [63] and SwissBioisosteres server [64].

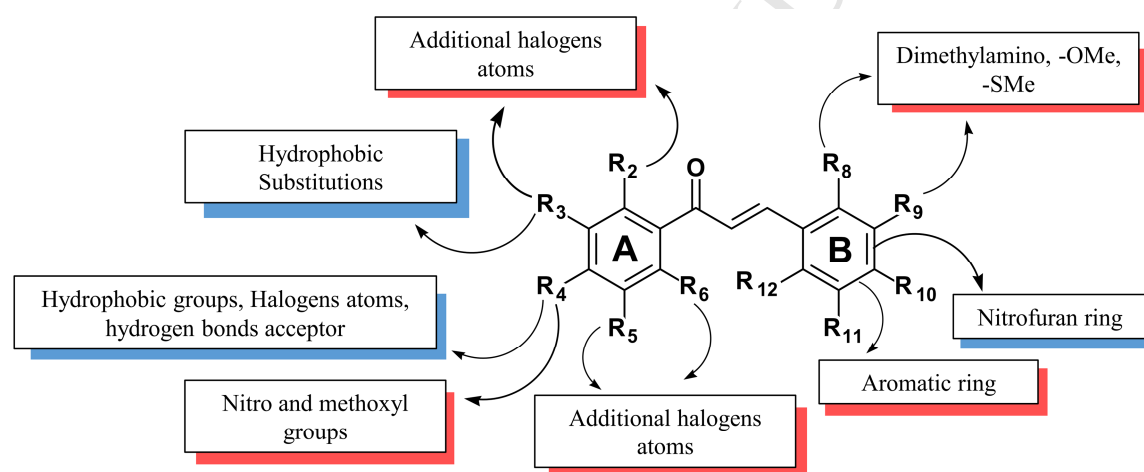


Figure 2. Derived SAR rules for chalcones with anti-TB activity. Modifications in blue shading increase the activity; with red – decrease the activity.

QSAR-DRIVEN design

QSAR modeling. MACCS [65], AtomPairs [66,67], Morgan [67,68], FeatMorgan [69], and Avalon fingerprints [70] combined with support vector machine (SVM) [71], gradient boosting machine (GBM) [72], and random forest (RF) [73] machine learning methods were used for the development of 15 different binary QSAR models. These models

were united in a consensus ensemble model (Table 1). The dataset was balanced prior to the modeling to keep the ratio of active to inactive compounds as 1:1. The results of 5-fold external cross-validation demonstrated high predictive power of the developed consensus model (Table 1). Ten rounds of Y-randomization were performed ($CCR \approx 0.5$, see Table S2, supplementary material) and indicated that developed models were not obtained due to chance correlations.

Table 1. Statistical characteristics of developed QSAR models estimated by 5-fold external CV.

Models	CCR	Kappa	Se	Sp	Coverage
MACCS-GBM	0.73	0.46	0.76	0.70	0.71
AtomPairs-GBM	0.71	0.41	0.71	0.70	0.71
Morgan-GBM	0.76	0.51	0.77	0.74	0.68
FeatMorgan-GBM	0.74	0.47	0.76	0.71	0.66
Avalon-GBM	0.74	0.47	0.79	0.68	0.77
MACCS-RF	0.75	0.51	0.79	0.72	0.71
AtomPairs-RF	0.75	0.50	0.73	0.77	0.71
Morgan-RF	0.76	0.52	0.79	0.73	0.68
FeatMorgan-RF	0.75	0.50	0.70	0.80	0.66
Avalon-RF	0.74	0.49	0.76	0.73	0.77
MACCS-SVM	0.77	0.53	0.77	0.76	0.71
AtomPairs-SVM	0.74	0.48	0.74	0.74	0.71
Morgan-SVM	0.76	0.53	0.80	0.73	0.68
FeatMorgan-SVM	0.76	0.51	0.75	0.76	0.66
Avalon-SVM	0.73	0.46	0.72	0.74	0.77
Consensus*	0.77	0.53	0.79	0.74	1.00

GBM: Gradient Boosting Machine; SVM: Support Vector Machine; RF: Random Forest; CCR: correct classification rate; Kappa: Cohen's kappa coefficient; Se: sensitivity; Sp: specificity. *Consensus model was developed by averaging the predictions of all 15 single models.

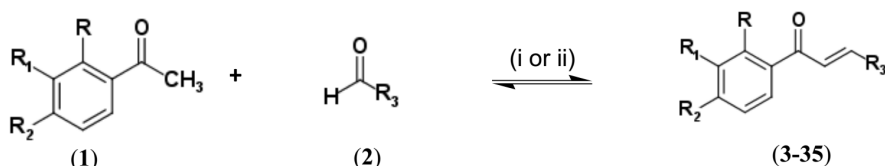
Then, the developed consensus model was used for virtual screening of the chalcones designed by bioisosteric replacement aiming at prioritizing the compounds for chemical synthesis. The chalcones obtained by bioisosteric replacement (Table S3) are drug-like

1 compounds and satisfy Veber [74] and Lipinski [75] rules. In addition, the designed
 2 compounds contained no PAINs substructures [76,77].

3 Chemistry

4 Based on the results of the *in silico* design, we synthesized the selected nitrofuran- **3-**
 5 **17**, nitrothiophene- **18-24** and chlorothiophene **25** containing chalcones (Scheme 1). The
 6 standard Claisen-Schmidt condensation [78] under basic condition could not be used because
 7 the starting materials (aldehydes, nitrofurans, nitrothiophenes, and chlorothiophenes) are
 8 alkali-sensitive. Thus, the modified Claisen-Schmidt condensation was performed using
 9 acetic acid as solvent and sulfuric acid as catalyst [79,80]. Compounds **26-35** were
 10 synthesized following standard Claisen-Schmidt condensation using 20% NaOH as catalyst
 11 [78] (see Experimental Section of the Supplementary material for details of spectra and purity
 12 data).

13 **Scheme 1.** Synthesis of aryl chalcones and heteroaryl chalcone derivatives.



(3) R = H, R₁ = H, R₂ = Br, R₃ = 5-nitrofuran

(4) R = H, R₁ = H, R₂ = Morpholine, R₃ = 5-nitrofuran

(5) R = H, R₁ = H, R₂ = Piperidine, R₃ = 5-nitrofuran

(6) R = H, R₁ = H, R₂ = Imidazole, R₃ = 5-nitrofuran

(7) R = H, R₁ = H, R₂ = *tert*-butyl, R₃ = 5-nitrofuran

(8) R = H, R₁ = H, R₂ = cyclohexyl, R₃ = 5-nitrofuran

(9) R = H, R₁ = H, R₂ = piperazine, R₃ = 5-nitrofuran

(10) R = H, R₁ = H, R₂ = phenyl, R₃ = 5-nitrofuran

(11) R = CH₃, R₁ = H, R₂ = H, R₃ = 5-nitrofuran

(12) R = H, R₁ = H, R₂ = *N*-butyl, R₃ = 5-nitrofuran

(13) R = H, R₁ = H, R₂ = I, R₃ = 5-nitrofuran

(14) R = H, R₁ = CH₃, R₂ = H, R₃ = 5-nitrofuran

(15) R = H, R₁ = H, R₂ = pyrrolidine, R₃ = 5-nitrofuran

(16) R = H, R₁ = Br, R₂ = H, R₃ = 5-nitrofuran

(17) R = H, R₁ = H, R₂ = CH₃, R₃ = 5-nitrofuran

(18) R = H, R₁ = H, R₂ = imidazole, R₃ = 5-nitrothiophene

(19) R = H, R₁ = H, R₂ = *tert*-butyl, R₃ = 5-nitrothiophene

(20) R = H, R₁ = H, R₂ = *N*-butyl, R₃ = 5-nitrothiophene

(21) R = H, R₁ = H, R₂ = cyclohexyl, R₃ = 5-nitrothiophene

(22) R = H, R₁ = H, R₂ = morpholine, R₃ = 5-nitrothiophene

(23) R = H, R₁ = H, R₂ = SCH₃, R₃ = 5-nitrothiophene

(24) R = H, R₁ = H, R₂ = CH₃, R₃ = 5-nitrothiophene

(25) R = H, R₁ = H, R₂ = Imidazole, R₃ = chlorothiophene

(26) R = H, R₁ = H, R₂ = piperidine, R₃ = 3-nitrophenyl

(27) R = H, R₁ = H, R₂ = phenyl, R₃ = *p*-dimethylaminophenyl

(28) R = H, R₁ = H, R₂ = phenyl, R₃ = *p*-methoxyphenyl

(29) R = H, R₁ = H, R₂ = CH₃, R₃ = furan

(30) R = H, R₁ = H, R₂ = I, R₃ = *p*-methoxyphenyl

(31) R = H, R₁ = H, R₂ = piperidine, R₃ = furan

(32) R = H, R₁ = H, R₂ = Br, R₃ = *p*-methoxyphenyl

(33) R = H, R₁ = H, R₂ = *tert*-butyl, R₃ = pyrrole

(34) R = CH₃, R₁ = H, R₂ = piperidine, R₃ = *p*-nitrophenyl

(35) R = H, R₁ = H, R₂ = *tert*-butyl, R₃ = furan

14

Reagents and conditions: (i) H₂SO₄ conc., AcOH, reflux, 100 °C, 4 – 24 h; (1) acetophenones, (2) nitrofuraldehyde or nitrothiophenecarboxaldehyde, (3-25) analogs nitrofurans or nitrothiophenes. (ii) 20% NaOH, EtOH, room temperature, 10 h; (1) acetophenones; (2) aromatics aldehydes; (26-35) phenyl analogs, furan or pyrrole.

Among designed and synthesized compounds, 17 compounds are new and were not published previously (6-9, 11, 14, 15, 17-23, 25, 31, and 33), and thirty compounds (6-35) were not tested against tuberculosis before.

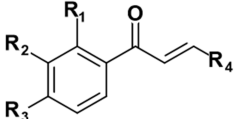
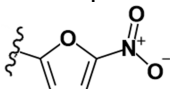
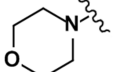
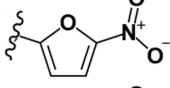
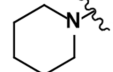
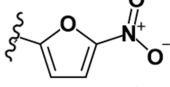
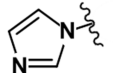
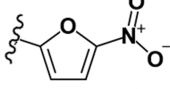
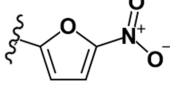
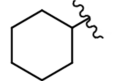
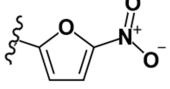
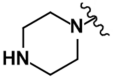
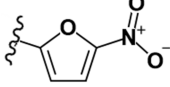
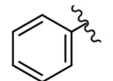
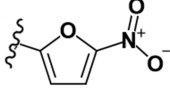
Antituberculosis activity

The compounds were submitted to biological assays against *M. tb.* H37Rv, under both *aerobic* (replicating) and *anaerobic* (non-replicating) conditions using MABA and LORA assays, respectively [81,82]. Minimum inhibitory concentrations (MICs) were defined as the lowest compound concentration effecting $\geq 90\%$ inhibition of fluorescence or luminescence, respectively. We evaluated 33 chalcones including three known compounds (Table 2) [79]. Twenty-two compounds had low MICs in both the MABA and LORA assays. Compounds containing substituents in the *para*-position of ring A, and containing nitrofurans and nitrothiophenes as ring B (Figure 2) were the most potent. *Ortho*- and *meta*-substituted compounds were somewhat less active. Ten designed compounds 4, 8, 9, 11, 13, 17-20, and 23 had MABA MICs of $< 1 \mu\text{M}$ and LORA MICs of $< 10 \mu\text{M}$ (Table 2). And four this compounds 9, 18, and 19 were more potent than (MIC = 0.27, 0.19, and 0.22 μM respectively) of standard drug INH (MIC = 0.41 μM) used on treatment of TB. Already the compound 23 exhibited MIC similar (0.45 μM) to INH.

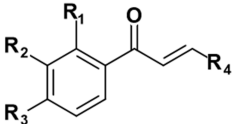
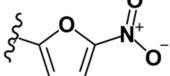
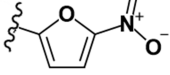
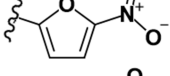
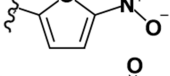
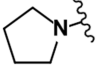
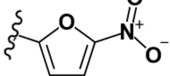
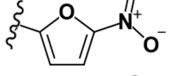
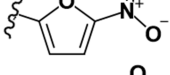
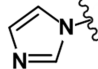
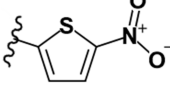
The most potent compound was the nitrothiophene analogue 18 with MABA MIC = 0.19 μM and LORA MIC = 1.73 μM . The substitution of furan ring by thiophene or nitro-substituted thiophene (e.g., 6 and 18) led to 5.5-fold increase of the activity in the MABA (1.05 μM to 0.19 μM) and 4-fold for LORA (6.94 μM to 1.73 μM). The compounds 19 and

1 **20** were the most active in MABA, however **20** lost activity in the LORA in comparison to its
2 nitrofurantoin analogue **12**. Nitrothiophenes **21** and **22**, unlike their nitrofurantoin analogues **8** and **4**,
3 were inactive (MIC>10 μ M) in both MABA and LORA assays.

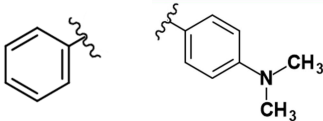
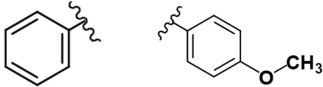
Table 2. *In vitro* antituberculosis activity reported in minimum inhibitory concentration (MIC, μM) (MABA and LORA), MABA MIC of selected compounds against isogenic monodrug-resistant *M. tb.*, rRMP and rINH, spectrum of activity and selectivity index of designed chalcones.

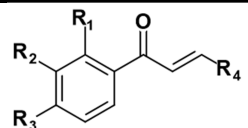
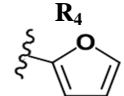
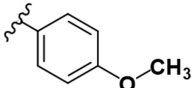
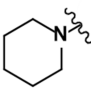
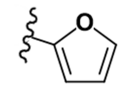
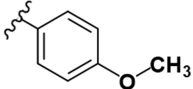
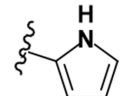
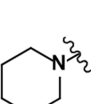
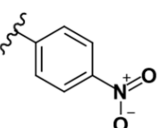
Code	Compounds				Minimum Inhibitory Concentration (μM)								SI
					MABA	LORA	rRMP	rINH	<i>C. alb.</i>	<i>E. coli</i>	<i>S. aureus</i>	<i>M. smeg.</i>	
	R ₁	R ₂	R ₃	R ₄									
3	H	H	Br		2.50±0.62	6.76±0.08	0.76±0.10	0.58±0.02	4.93±2.10	>10	0.36±0.11	7.12±0.06	ND
4	H	H			0.81±0.02	9.85±2.93	0.55±0.02	0.11±0.07	>10	>10	1.19±0.46	>10	123
5	H	H			3.42±0.43	10.91±3.27	0.07±0.04	<0.03	>10	>10	>10	>10	ND
6	H	H			1.05±0.29	6.94±0.05	1.19±1.02	1.44±1.05	>10	3.18±1.10	0.34±0.10	>10	94
7	H	H	-C(CH ₃) ₃		0.35±0.11	>10	0.29±0.16	0.22±0.14	>10	>10	>10	>10	284
8	H	H			0.81±0.04	3.33±0.72	1.12±0.03	1.23±0.06	>10	>10	>10	>10	122
9	H	H			0.27±0.06	9.67±2.63	0.76±0.08	0.19±0.04	>10	>10	>10	>10	359
10	H	H			3.91±1.95	3.18±0.04	3.45±1.05	0.29±0.08	>10	>10	>10	>10	25

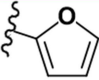
MABA: Microplate Alamar Blue Assay; LORA: Low Oxygen Recovery Assay; rRMP: monoresistant to rifampin; rINH: monoresistant to isoniazid. SI: Selectivity Index (Vero Cell IC₅₀/MABA MIC). *C. alb.*: *Candida albicans*; *M. smeg.*: *Mycobacterium smegmatis*.

Code	Compounds				Minimum Inhibitory Concentration (μM)								SI
					MABA	LORA	rRMP	rINH	<i>C. alb.</i>	<i>E. coli</i>	<i>S. aureus</i>	<i>M. smeg.</i>	
	R ₁	R ₂	R ₃	R ₄									
11	-CH ₃	H	H		0.57±0.01	4.59±0.01	1.08±0.04	1.07±0.03	6.36±0.09	>10	1.09±0.08	9.50±0.01	41
12	H	H	(CH ₂) ₃ CH ₃		1.31±1.01	4.21±0.22	4.70±0.45	2.23±1.02	>10	>10	2.23±0.00	>10	57
13	H	H	-I		0.60±0.34	4.12±0.14	1.18±0.25	1.08±0.09	>10	>10	>10	4.62	166
14	H	-CH ₃	H		1.27±0.04	4.75±0.18	3.78±1.31	1.93±0.08	>10	>10	2.23±0.00	>10	43
15	H	H			>10	4.30±0.00	-	-	>10	>10	>10	>10	ND
16	H	-Br	H		1.32±0.45	5.65±2.22	1.88±0.30	1.12±1.98	>10	>10	1.68±0.29	4.84±0.10	52
17	H	H	-SCH ₃		0.66±0.06	5.07±1.03	0.24±0.07	0.80±0.06	>10	>10	0.58±0.08	4.81±0.01	61
18	H	H			0.19±0.15	1.73±0.21	0.60±0.10	0.30±0.06	>10	>10	0.28±0.30	4.39±0.05	225

19	H	H	-C(CH ₃) ₃		0.22±0.13	4.18±0.55	0.14±0.01	0.15±0.05	>10	>10	>10	>10	454
Code	Compounds				Minimum Inhibitory Concentration (μM)								SI
					MABA	LORA	rRMP	rINH	<i>C. alb.</i>	<i>E. coli</i>	<i>S. aureus</i>	<i>M. smeg.</i>	
	R ₁	R ₂	R ₃	R ₄									
20	H	H	-(CH ₂) ₃ CH ₃		0.54±0.31	5.56±0.66	0.48±0.00	0.31±0.02	>10	>10	>10	>10	81
21	H	H			>10	5.75±0.01	-	-	>10	>10	>10	>10	ND
22	H	H			>10	>10	-	-	>10	>10	>10	>10	ND
23	H	H	-SCH ₃		0.45±0.20	5.96±2.47	0.14±0.03	0.22±0.01	>10	>10	>10	>10	222
24	H	H	-CH ₃		1.87±0.31	2.05±0.37	1.21±0.01	0.96±0.04	>10	>10	>10	>10	ND
25	H	H			9.29±0.45	9.75±0.63	8.89±2.03	9.03±1.80	>10	>10	>10	>10	ND
26	H	H			>10	>10	-	-	>10	>10	>10	>10	ND

27	H	H		>10	>10	-	-	>10	>10	>10	>10	ND
28	H	H		>10	>10	-	-	>10	>10	1.18±0.40	>10	ND

Code	Compounds				Minimum Inhibitory Concentration (μM)								SI
					MABA	LORA	rRMP	rINH	<i>C. alb.</i>	<i>E. coli</i>	<i>S. aureus</i>	<i>M. smeg.</i>	
	R ₁	R ₂	R ₃	R ₄									
29	H	H	-SCH ₃		>10	>10	-	-	>10	>10	>10	>10	ND
30	H	-I	H		4.90±1.83	>10	8.31±1.01	7.75±0.08	>10	>10	>10	>10	20
31	H	H			>10	>10	-	-	>10	>10	>10	>10	ND
32	H	-Br	H		8.54±2.07	8.20±1.60	9.28±2.01	4.94±1.92	>10	>10	>10	>10	11
33	H	H	-C(CH ₃) ₃		>10	>10	-	-	>10	>10	>10	>10	ND
34	H	H			>10	>10	-	-	>10	>10	>10	>10	ND

35	H	H	-C(CH ₃) ₃		>10	>10	-	-	>10	>10	>10	>10	ND
RMP					0.05	0.19	>1	-	-	-	-	>10	2000
INH					0.41	>256	-	>5	-	-	-	>10	
Amph.B					-	-	-	-	<0.004	-	-	-	
Amp					-	-	-	-	-	1.18	0.25	-	

MABA: Microplate Alamar Blue Assay; LORA: Low Oxygen Recovery Assay; rRMP: monoresistant to rifampin; rINH: monoresistant to isoniazid. SI: Selectivity Index (Vero Cell IC₅₀/MABA MIC). RMP: rifampin, INH: isoniazid, Amph. B: amphotericin B, Amp.: ampicillin

Cytotoxicity assay

To verify the possibility that the anti-TB activity of the designed compounds arises from general toxicity, Vero cells were used to estimate the *in vitro* cytotoxicity of the 18 most potent compounds in MABA and LORA assays. These compounds demonstrated modest to high selectivity on this assay, with selectivity indices (SI) ranging between 11 and 454 (Table 2).

Spectrum of activity

We also investigated selectivity of compounds with respect to activity against *Candida albicans*, *Escherichia coli*, *Staphylococcus aureus*, and *M. smegmatis* (Table 2). Most of the tested compounds had MIC >10 μ M, except **3**, **4**, **6**, **11-14**, **16-18**, **20**, and **28** that exhibited MICs against *S. aureus* of 0.28-2.23 μ M.

Conversely, these compounds demonstrated broad-spectrum activity against non-tuberculosis mycobacterias (NTMs), i.e., *M. abscessus*, *M. chelonae*, *M. marinum*, *M. avium*, *M. kansasii*, and *M. bovis* (Table S3). Compounds **3**, **8-13**, **15-25**, **30**, and **32** had MICs <10 μ M against *M. avium*, *M. kansasii*, and *M. bovis*, and compound **10** demonstrated MICs of 0.14 μ M and 0.08 μ M against *M. kansasii* and *M. bovis*, respectively.

Evaluation in *M. tb.* resistant strains

We evaluated the subset of most potent compounds (**3-14**, **16-21**, **24** and **25**) against rifampin- and isoniazid-resistant strains of *M. tb.* H37Rv (Table 2). All tested compounds were potent against resistant strains (MIC < 10 μ M), and compounds **3-5**, **7**, **9**, and **17-21** exhibit MIC < 1 μ M against resistant strains. Compound **5** was the most potent compound with MIC of 0.07 μ M against rRMP and < 0.03 μ M against rINH strains, indicating that this compound is promising for RMP and INH resistant strains.

CONCLUSIONS

The integration of *in silico* design, QSAR-driven virtual screening, synthesis, and experimental evaluation in a single pipeline led to discovery of new and promising anti-TB compounds. After the compilation of the initial dataset and its rigorous curation, the specific SAR rules were developed and used for designing of new chalcones by bioisosteric replacement. For instance, hydrophobic groups and H-bond acceptors are preferred in the *para*-position of ring A combined with nitrofurane or nitrothiophene serving as ring B. Then, the developed consensus QSAR model of antimicrobial activity was applied for virtual screening and prioritization of designed compounds. Thirty-three chalcone derivatives were synthesized, structures were confirmed by spectroscopic methods and tested against normoxic, replicating (MABA), and hypoxic, non-replicating (LORA) cultures of *M. tb*.

We identified 20 compounds with MIC <10 μ M in MABA including 10 compounds (**4**, **8**, **9**, **11**, **13**, **17-20**, and **23**) with MIC < 1 μ M in MABA and < 10 μ M in LORA. All tested compounds were also active against *M. tb* resistant strains to isoniazid or rifampicin. The compounds were mostly inactive against all other tested bacteria strains and against mammalian (VERO) cells. Therefore, those compounds are selective for the genus *Mycobacteria* with moderate activity against *S. aureus*. Our compounds satisfy the criteria for developing new anti-TB hits published by Katsuno and coauthors[83] and due to their high potency and activity against resistant strains. Therefore, the designed and synthesized chalcones and heterochalcones could serve as perspective starting points for the development of anti-tubercular agents.

EXPERIMENTAL SECTION

Computational Design

Dataset. We retrieved 604 chalcone and heteroaryl chalcone compounds with experimental data tested against *M. tb.* H37Rv from the PubChem (AID: 1626 and AID: 1949) [51], ChEMBL [52], SciFinder [53], and from the literature. Compounds that had inconclusive IC₅₀ values were considered unreliable and were not included in the modeling.

Data curation. The compiled dataset of 604 compounds was carefully curated following the protocols proposed by Fourches et al.[54–56] Briefly, explicit hydrogens were added, whereas specific chemotypes such as aromatic and nitro groups were normalized using ChemAxon Standardizer (v.15.1.26.0, ChemAxon, Budapest, Hungary, <http://www.chemaxon.com>). Polymers, inorganic salts, organometallic compounds, mixtures, and duplicates were removed. Modeling-ready curated dataset contained 571 compounds.

SAR analysis. SAR analysis was performed using the MMP (Matched Molecular Pairs) approach [84], Structural similarity was calculated using Tanimoto coefficient obtained on MACCS keys.

SAR analysis and bioisosteric replacement. SAR analysis was performed using the MMP (Matched Molecular Pairs) approach [84]. Structural similarity was calculated using Tanimoto coefficient [85] obtained on MACCS keys. Bioisosteric replacement was performed in the *p*-substituents on the ring A (Figure 1), i.e., piperidine of the most active chalcone (MIC = 0.19 μ M), (2E)-3-(5-nitrofuran-2-yl)-1-[4-(piperidin-1-yl)phenyl]prop-2-en-1-one, described in literature [79]. Design of these bioisosters were performed using BROOD v.2.0 software [63] and SwissBioisosteres webserver (<http://www.swissbioisostere.ch>) [64].

Molecular fingerprints. Five different types of fingerprints were used: molecular access system (MACCS) structural key fingerprints [65], AtomPair [66,67], Morgan, [67,68]

FeatMorgan, [69] and Avalon.[70] All fingerprints were calculated using the open-source cheminformatics toolkit RDKit v.2.4.0 [86].

Dataset analysis and under-sampling. The curated dataset was unbalanced (148 active and 423 inactive compounds), which is not recommended to build binary QSAR models. Therefore, we decided to balance the dataset using linear under-sampling strategy developed by Braga, R.C. (Neves et al, 2016) [87]. Unlike the traditional under-sampling methods which randomly balance the dataset, this strategy retains the most representative inactive compounds in the balanced dataset, thus assuring as high as possible coverage of original chemical space. As a result, balanced dataset containing 148 active and 148 inactive compounds was used for the modeling.

Machine learning techniques. SVM[71], GBM [72], and Random Forest (RF) [73], approaches implemented in R v.3.0.3 [88] were used for the building and optimization of statistically acceptable QSAR models. All machine learning classifiers were implemented using the R v.3.0.3 [88]. More details about these machine modeling techniques are given in Supplementary material.

External validation of developed QSAR models. 5-fold external cross-validation is the standard approach for the estimation of predictive power of QSAR models [89]. In this procedure, the dataset is randomly divided in five subsets of equal size (20% of compounds each). One of these subsets serve as an external validation fold and the other four subsets are used building of the model. The same procedure is repeated five times to place each compound once in the corresponding external fold. Then, the predictivity of the models is estimated based on these external folds. Description of statistical characteristics used for estimation of robustness and external predictivity of developed models is provided in supplementary material.

Consensus modeling. The underlying idea of consensus predictions is that an implicit SAR for a given dataset can be formally manifested by a variety of QSAR models built with different types of molecular descriptors and diverse machine learning approaches. Rigorously built individual models form an ensemble that allows for consensus bioactivity prediction using all models at once. The development of consensus models is generally recommended because usually they result in better predictivity and better coverage of chemical space during virtual screening [90]. To obtain consensus prediction, we have averaged the predictions of all individual models.

Chemical synthesis

All the chemicals and solvents were purchased from Sigma Aldrich[®]. The progress of all reactions was monitored on Merck KGaA precoated silica gel plates 0.25 mm (with fluorescence indicator UV₂₅₄) using ethyl acetate/n-hexane as solvent system. Spots were visualized by irradiation with ultraviolet light (254 nm). Melting points (mp) were determined using open capillary method on Melting Point III Marte[®] apparatus. Proton (¹H) and (¹³C) NMR spectra were recorded on Bruker Avance 400 spectrometer at 400 MHz for ¹H and 100 MHz for ¹³C using DMSO-*d*₆ and CDCl₃ as solvents referenced. Chemical shifts are given in parts per million (ppm) (δ relative to residual solvent peak for ¹H and ¹³C). Spectra Mass was performed on a LCMS-2020 Liquid Chromatograph Mass Spectrometer Shimadzu, the column was Agilent XDB-C18, 35 μ M, 21x20 nm. IR spectra were recorded on a PerkinElmer model Spectrum 400 (medium, sweep of 4000 to 400 cm⁻¹). Synthesized compounds were \geq 96% pure as determined by high performance liquid chromatography (HPLC) Shimadzu with PDA detector, Nucleodur 100-5 CN-RP column 205x4.6mm, mobile phase water/0.1% TFA and acetonitrile with flow of 1 mL/min.

For the synthesis of **3-25**, substituted acetophenones (0.5 equiv, 0.5 mmol) and nitroaromatics (0.5 equiv., 0.5 mmol) were dissolved in acetic acid (1 mL) and concentrated

sulfuric acid (0.05 mL) and were stirred at 100° C until completion of the reaction (4-24 h). The cooled mixture and the solid was washed with iced methanol (200 mL) for purification. For the synthesis of **26-35**, 0.4 mL of aqueous NaOH (20% w/v) was added to the solution of the acetophenones substituted in 4' position (1 mmol) in EtOH. The resulting mixture was stirred at the room temperature for 10 hours. The formed precipitate was filtered and washed with cold water. If no precipitation occurred, the resulting mixture was neutralized with 5% HCl filtered and dried. The crude was then subjected to chromatography column with EtOAc/Hexane (7:3, v/v) as eluent.

(2E)-1-(4-bromophenyl)-3-(5-nitrofuran-2-yl)prop-2-en-1-one (LabMol-63) 3. Yellow solid; yield 33% (107 mg, 0.33 mmol); mp 182°C; HPLC purity 98.13%. ¹H NMR (CDCl₃): δ = 7.95 (d, 2H, *J* = 8.0 Hz), 7.70 (d, 2H *J* = 8.0 Hz), 7.72 (d, 1H, *J* = 15.0 Hz), 7.58 (d, 1H, *J* = 15.0 Hz), 7.39 (d, 1H, *J* = 4.0 Hz), 6.87 (d, 1H, *J* = 4.0 Hz). ¹³C NMR (CDCl₃): δ = 187.1, 152.4, 135.4, 131.8 (2 C), 130.4, 129.7 (2 C), 128.5, 128.1, 123.9, 116.4, 112.7. IR (KBr): ν = 1663 (s; ν (C=O)), 1607 (s; ν (C=C_{αβ})), 1475, 1301 (s; ν (Ar-NO₂)).

(2E)-1-[4-(morpholin-4-yl)phenyl]-3-(5-nitrofuran-2-yl)prop-2-en-1-one (LabMol-64) 4. Red solid, yield 13% (42 mg, 0.12 mmol); mp 86°C; HPLC purity 98.19%. ¹H NMR ([D₆] DMSO): δ = 8.02 (d, 2H, *J* = 8.0 Hz), 7.88 (d, 1H, *J* = 15.0 Hz), 7.80 (d, 1H, *J* = 3.6 Hz), 7.51 (d, 1H, *J* = 15.0 Hz), 7.42 (d, 1H, *J* = 3.6 Hz), 7.04 (d, 2H, *J* = 9.2 Hz), 3.73 (m, 4H), 3.41 (m, 4H). ¹³C NMR ([D₆] DMSO): δ = 185.2, 154.1, 153.8, 130.8 (2 C), 127.1, 126.6, 125.6, 116.9, 114.9, 113.1 (2 C), 65.8 (2 C), 46.6 (2 C). IR (KBr): ν = 1660 (s; ν (C=O)), 1601 (s; ν (C=C_{αβ})), 1515, 1355 (s; ν (Ar-NO₂)), 1238 (s; ν (C-N)), 1119 (s; ν (C-O)). ESI (+)-MS (MeOH): *m/z* = 329 [M+H]⁺

(2E)-3-(5-nitrofuran-2-yl)-1-[4-(piperidin-1-yl)phenyl]prop-2-en-1-one (LabMol-65) 5. Red solid, yield 17% (56 mg, 0.17 mmol); mp 220°C; HPLC purity 98.41%. ¹H NMR ([D₆]

1 DMSO): δ = 7.97 (d, 2H, J = 9.2 Hz), 7.86 (d, 1H, J = 15.0 Hz), 7.80 (d, 1H, J = 4.0 Hz),
 2 7.44 (d, 1H, J = 15.0 Hz), 7.40 (d, 1H, J = 4.0 Hz), 6.99 (d, 2H, J = 9.2 Hz), 4.43 (s, 4H),
 3 1.60 (s, 6H). ^{13}C NMR ($[\text{D}_6]$ DMSO): δ = 184.9, 154.1, 153.9, 131.0 (2 C), 126.7, 125.8,
 4 125.3, 116.8, 115.0, 112.9 (2 C), 47.6 (2 C), 24.9 (2 C), 24.0. IR (KBr): ν = 1642 (s, $\nu(\text{C}=\text{O})$),
 5 1607 (s; $\nu(\text{C}=\text{C}_{\alpha\beta})$), 1578, 1354 (s, $\nu(\text{Ar}-\text{NO}_2)$), 1235 (s; $\nu(\text{C}-\text{N})$). ESI (+)-MS (MeOH): m/z
 6 = 327 $[\text{M}+\text{H}]^+$

7 **(2E)-1-[4-(1H-imidazol-1-yl)phenyl]-3-(5-nitrofuran-2-yl)prop-2-en-1-one (LabMol-66)**

8 **6.** Brown solid; yield 12% (36 mg, 0.12 mmol); mp 232°C; HPLC purity 99.08%. ^1H NMR
 9 ($[\text{D}_6]$ DMSO): δ = 9.07 (s, 1H); 8.32 (d, 2H, J = 8.0 Hz), 8.15 (s, 1H), 7.97 (d, 2H, J = 8.0
 10 Hz), 7.94 (d, 1H, J = 16.0 Hz), 7.83 (d, 1H, J = 4.0 Hz), 7.63 (d, 1H, J = 16.0 Hz), 7.52 (s,
 11 1H), 7.48 (d, 1H, J = 4.0 Hz). ^{13}C NMR ($[\text{D}_6]$ DMSO): δ = 187.2, 153.2, 152.1, 139.6, 135.9,
 12 135.8, 130.7 (2 C), 129.0, 126.3, 121.0 (2 C), 119.2, 118.0, 114.9. IR (KBr): ν = 1662 (s;
 13 $\nu(\text{C}=\text{O})$), 1609 (s; $\nu(\text{C}=\text{C}_{\alpha\beta})$), 1566, 1352 (s, $\nu(\text{Ar}-\text{NO}_2)$). ESI (+)-MS (MeOH): m/z = 310
 14 $[\text{M}+\text{H}]^+$

15 **(2E)-1-(4-tert-butylphenyl)-3-(5-nitrofuran-2-yl)prop-2-en-1-one (LabMol-68) 7.** Yellow

16 solid; yield 22% (67 mg, 0.22 mmol); mp 180°C; HPLC purity 99.89%. ^1H NMR (CDCl_3): δ
 17 = 1.37 (s, 9H), 6.84 (d, 1H, J = 4.0 Hz), 7.39 (d, 1H, J = 4.0 Hz), 7.55 (d, 1H, J = 15.0 Hz),
 18 7.55 (d, 2H, J = 8.4Hz), 7.77 (d, 1H J = 15.0Hz), 8.01 (d, 2H, J = 8.4Hz). ^{13}C NMR (CDCl_3):
 19 δ = 188.3, 157.2, 152.8, 151.8, 134.2, 128.2 (2 C), 127.3, 125.4 (2 C), 124.8, 115.8, 112.8,
 20 34.8, 30.6 (3 C). IR (KBr): ν = 1651 (s; $\nu(\text{C}=\text{O})$), 1596 (s; $\nu(\text{C}=\text{C}_{\alpha\beta})$), 1527, 1354 (s, $\nu(\text{Ar}-$
 21 $\text{NO}_2)$), 1391 (m, $\nu(\text{CH}_3)$). ESI (+)-MS (MeOH): m/z = 300 $[\text{M}+\text{H}]^+$

22 **(2E)-1-(4-cyclohexylphenyl)-3-(5-nitrofuran-2-yl)prop-en-2-one (LabMol-72) 8.** Yellow

23 solid; yield 44% (72 mg, 0.22 mmol); mp 162° C; HPLC purity 98.59%. ^1H NMR (CDCl_3): δ
 24 = 8.00 (d, 2H, J = 8.0 Hz), 7.77 (d, 1H, J = 15.6 Hz), 7.54 (d, 1H, J = 15.6 Hz), 7.38 (d, 1H, J

1 = 3.6 Hz), 7.37 (d, 2H, $J = 8.0$ Hz), 6.84 (d, 1H, $J = 3.6$ Hz), 2.61 (s, 1H); 2.18 (s, 2H); 1.89
 2 (s, 2H), 1.78 (s, 1H), 1.39 (m, 6H). ^{13}C NMR (CDCl_3): 187.7, 154.1 (2 C), 152.9, 134.6,
 3 128.5 (2 C), 127.3, 127.0 (2 C), 124.8, 115.8, 112.8, 44.3, 33.6 (2 C), 26.3 (2 C), 25.6. IR
 4 (KBr): $\nu = 2925$ (s; $\nu(\text{C-H})$), 1651 (s; $\nu(\text{C=O})$), 1593 (s; $\nu(\text{C=C}_{\alpha\beta})$), 1526, 1353 (s, $\nu(\text{Ar-NO}_2)$),
 5 1481 (m, $\nu(\text{CH}_2)$). ESI (+)-MS (MeOH): $m/z = 326$ $[\text{M}+\text{H}]^+$.

6 **(2E)-3-(5-nitrofuran-2-yl)-1-[4-(piperazin-1-yl)phenyl]prop-2-en-1-one (LabMol-73) 9.**

7 Red solid; yield 42% (59 mg, 0.12 mmol); mp 221°C ; HPLC purity 98.07%. ^1H NMR
 8 (CDCl_3): $\delta = 8.00$ (d, 2H, $J = 8.8$ Hz), 7.79 (d, 1H, $J = 15.2$ Hz), 7.51 (d, 1H, $J = 15.2$ Hz),
 9 7.38 (d, 1H, $J = 4.0$ Hz), 6.90 (d, 2H, $J = 8.8$ Hz), 6.78 (d, 1H, $J = 4.0$ Hz), 3.44 (s, 4H), 1.69
 10 (s, 5H). ^{13}C NMR (CDCl_3): δ 185.2, 154.2 (2 C), 153.5, 130.8 (2 C), 125.9, 125.7, 125.3,
 11 115.1, 112.9, 112.7 (2 C), 47.9 (2 C), 24.9 (2 C), 23.9. IR (KBr) $\nu = 1618$ (s; $\nu(\text{C=O})$), 1609
 12 (s; $\nu(\text{C=C}_{\alpha\beta})$), 1580, 1354 (s, $\nu(\text{Ar-NO}_2)$), 1513 (m, $\nu(\text{N-H})$), HR-MS (m/z) (ESI): calcd for
 13 $\text{C}_{17}\text{H}_{18}\text{N}_3\text{O}_4$ $[\text{M} + \text{H}]^+$: 328.1291; found: 328.1289.

14 **(2E)-3-(5-nitrofuran-2-yl)-1-(4-phenylphenyl)prop-2-en-1-one (LabMol-74) 10.** Yellow

15 solid; yield 62% (100 mg, 0.31 mmol); mp 200°C ; HPLC purity 99.29%. ^1H NMR (CDCl_3):
 16 $\delta = 8.16$ (d, 2H, $J = 8.4$ Hz), 7.83 (d, 1H, $J = 15.5$ Hz), 7.77 (d, 2H, $J = 8.4$ Hz), 7.67 (d, 2H,
 17 $J = 7.2$ Hz), 7.59 (d, $J = 15.5$ Hz, CH α , 1H), 7.50 (s, 2H); 7.44 (d, 1H, $J = 7.2$ Hz), 7.40 (s,
 18 1H), 6.86 (s, 1H). ^{13}C NMR (CDCl_3): $\delta = 187.6$, 152.7 (2 C), 145.9, 139.2, 135.4, 128.0 (2
 19 C), 128.6 (2 C), 128.0, 127.6, 127.1 (2 C), 126.9 (2 C), 124.6, 116.1, 112.8. IR (KBr): $\nu =$
 20 1660 (s; $\nu(\text{C=O})$), 1598 (s; $\nu(\text{C=C}_{\alpha\beta})$), 1597, 1352 (s, $\nu(\text{Ar-NO}_2)$), 1513, 1474 (s, $\nu(\text{ArC=C})$).
 21 ESI (+)-MS (MeOH): $m/z = 320$ $[\text{M}+\text{H}]^+$.

22 **(2E)-1-(2-methylphenyl)-3-(5-nitrofuran-2-yl)prop-2-en-1-one (LabMol-75) 11.** Yellow

23 solid; yield 9% (12 mg, 0.04 mmol); mp 114°C ; HPLC purity 99.20%. ^1H NMR (CDCl_3): δ
 24 = 7.61 (s, 1H), 7.44 (s, 1H), 7.41 (s, 1H), 7.35 (s, 1H), 7.37 (d, 1H, $J = 3.6$ Hz), 7.31 (s, 2H),

6.83 (d, 1H, $J = 3.6$ Hz), 2.50 (s, 3H). ^{13}C NMR (CDCl_3): $\delta = 193.0, 152.5, 137.6, 137.3, 131.4, 131.1, 128.7, 128.2, 127.9, 125.3, 115.7, 112.7$ (2 C), 20.2. IR (KBr): $\nu = 1663$ (s; $\nu(\text{C}=\text{O})$), 1608 (s; $\nu(\text{C}=\text{C}_{\alpha\beta})$), 1483, 1348 (s, $\nu(\text{Ar}-\text{NO}_2)$), 1476 (s, $\nu(\text{CH}_3)$). ESI (+)-MS (MeOH): $m/z = 258$ $[\text{M}+\text{H}]^+$, HR-MS (m/z) (ESI): calcd for $\text{C}_{14}\text{H}_{12}\text{NO}_4$ $[\text{M} + \text{H}^+]$: 258.0760; found: 258.0770.

(2E)-1-(4-butylphenyl)-3-(5-nitrofuran-2-yl)prop-2-en-1-one (LabMol-77) 12. Yellow solid, yield 10% (16 mg, 0.05 mmol); mp 100°C ; HPLC purity 97.93%. ^1H NMR (CDCl_3): $\delta = 8.00$ (d, 2H, $J = 8.4$ Hz), 7.78 (d, 1H, $J = 15.6$ Hz), 7.55 (d, 1H, $J = 15.6$ Hz), 7.39 (d, 1H, $J = 4.0$ Hz), 7.35 (d, 2H, $J = 8.4$ Hz), 6.84 (d, 1H, $J = 4.0$ Hz), 2.71 (t, 2H, $J = 8.0$ Hz), 1.65 (q, 2H, $J = 8.0$ Hz), 1.39 (s, 2H, $J = 8.0$ Hz), 0.95 (t, 3H, $J = 8.0$ Hz). ^{13}C NMR (CDCl_3): $\delta = 188.5, 161.5, 145.1, 140.8, 139.9, 136.9, 130.0$ (2 C), 129.8, 127.1, 126.9, 118.6, 114.1 (2 C), 94.0, 55.0. IR (KBr): $\nu = 2934$ (s; $\nu(\text{C}-\text{H})$), 1652 (s; $\nu(\text{C}=\text{O})$), 1607 (s; $\nu(\text{C}=\text{C}_{\alpha\beta})$), 1594, 1351 (s; $\nu(\text{Ar}-\text{NO}_2)$), 1481 (s; $\nu(\text{CH}_3)$), 810 (s; $\nu(\text{CH}_2)$). ESI (+)-MS (MeOH): $m/z = 300$ $[\text{M}+\text{H}]^+$, HR-MS (m/z) (ESI): calcd for $\text{C}_{17}\text{H}_{18}\text{NO}_4$ $[\text{M} + \text{H}^+]$: 300.1230; found: 300.1235.

(2E)-1-(4-iodophenyl)-3-(5-nitrofuran-2-yl)prop-2-en-1-one (LabMol-78) 13. Brown solid; yield 33% (61 mg, 0.16 mmol); mp 194°C ; HPLC purity 99.49%. ^1H NMR (CDCl_3): $\delta = 7.91$ (d, 2H, $J = 8.4$ Hz), 7.78 (d, 2H, $J = 8.4$ Hz), 7.70 (d, 1H, $J = 15.6$ Hz), 7.57 (d, 1H, $J = 15.6$ Hz), 7.39 (d, 1H, $J = 4.0$ Hz), 6.87 (d, 1H, $J = 4.0$ Hz). ^{13}C NMR (CDCl_3): $\delta = 187.4, 152.4$ (2 C), 137.8 (2 C), 136.0, 129.5 (2 C), 128.1, 123.9, 116.4, 112.7, 101.4. IR (KBr): $\nu = 1658$ (s; $\nu(\text{C}=\text{O})$), 1606 (s; $\nu(\text{C}=\text{C}_{\alpha\beta})$), 1579, 1351 (s; $\nu(\text{Ar}-\text{NO}_2)$).

(2E)-1-(3-methylphenyl)-3-(5-nitrofuran-2-yl)prop-2-en-1-one (LabMol-79) 14. Yellow solid; yield 17% (22 mg, 0.08 mmol); mp 141°C ; HPLC purity 97.92%. ^1H NMR (CDCl_3): $\delta = 7.86$ (s, 2H); 7.76 (d, 1H, $J = 15.6$ Hz), 7.55 (d, 1H, $J = 15.6$ Hz), 7.45 (s, 2H), 7.39 (d,

1H, $J = 4.0$ Hz), 6.85 (d, 1H, $J = 4.0$ Hz), 2.48 (s, 3H). ^{13}C NMR (CDCl_3): $\delta = 188.3, 152.8, 138.4, 138.8, 134.0, 128.7, 128.3, 127.5, 125.5, 124.8, 116.0, 112.8$ (2 C), 20.2. IR (KBr): $\nu = 3131$ (s; $\nu(\text{C-H})$) 1661 (s; $\nu(\text{C=O})$), 1606 (s; $\nu(\text{C=C}_{\alpha\beta})$), 1579, 1349 (s; $\nu(\text{Ar-NO}_2)$). ESI (+)-MS (MeOH): $m/z = 258$ $[\text{M}+\text{H}]^+$, HR-MS (m/z) (ESI): calcd for $\text{C}_{14}\text{H}_{12}\text{NO}_4$ $[\text{M} + \text{H}^+]$: 258.0760; found: 258.0764.

(2E)-3-(5-nitrofuran-2-yl)-1-[4-(pyrrolidin-1-yl)phenyl]prop-2-en-1-one (LabMol-81) 15.

Red solid; yield 36% (57 mg, 0.18 mmol); mp 242°C ; HPLC purity 96.87%. ^1H NMR (CDCl_3): $\delta = 8.03$ (d, 2H, $J = 8.8$ Hz), 7.82 (d, 1H, $J = 15.6$ Hz), 7.52 (d, 1H, $J = 15.6$ Hz), 7.38 (d, 1H, $J = 4.0$ Hz), 6.77 (d, 1H, $J = 3.6$ Hz), 6.59 (d, 2H, $J = 8.8$ Hz), 3.42 (s, 4H); 2.07 (s, 4H). ^{13}C NMR (CDCl_3): $\delta = 185.0, 153.6, 151.1, 130.9$ (2 C), 125.6, 125.5, 124.3, 114.9, 113.0, 110.7 (2 C), 42.2 (2 C), 24.0 (2 C). IR (KBr): $\nu = 2854$ (s; $\nu(\text{C-H})$), 1643 (s; $\nu(\text{C=O})$), 1610 (s; $\nu(\text{C=C}_{\alpha\beta})$), 1578, 1354 (s; $\nu(\text{Ar-NO}_2)$) 1199 (s; $\nu(\text{C-N})$). ESI (+)-MS (MeOH): $m/z = 313$ $[\text{M}+\text{H}]^+$

(2E)-1-(3-bromophenyl)-3-(5-nitrofuran-2-yl)prop-2-en-1-one (LabMol-82) 16. Brown

solid, yield 32% (62 mg, 0.19 mmol); mp 158°C ; HPLC purity 99.98%. ^1H NMR (CDCl_3): $\delta = 8.18$ (s, 1H); 7.98 (d, 1H, $J = 7.6$ Hz), 7.76 (d, 1H, $J = 8.0$ Hz), 7.69 (d, 1H, $J = 15.6$ Hz), 7.57 (d, 1H, $J = 15.6$ Hz), 7.44 (t, 1H, $J_1 = 7.6\text{Hz}, J_2 = 8.0$ Hz), 7.39 (d, 1H, $J = 4.0$ Hz), 6.88 (d, 1H, $J = 4.0$ Hz). ^{13}C NMR (CDCl_3): $\delta = 186.9, 152.3, 151.9, 138.5, 136.0, 131.2, 130.0, 128.4, 126.7, 123.9, 122.8, 116.5, 112.7$. IR (KBr): $\nu = 1664$ (s; $\nu(\text{C=O})$), 1607 (s; $\nu(\text{C=C}_{\alpha\beta})$), 1566, 1354 (s; $\nu(\text{Ar-NO}_2)$). ESI (+)-MS (MeOH): $m/z = 321$ $[\text{M}+\text{H}]^+$; HR-MS (m/z) (ESI): calcd for $\text{C}_{13}\text{H}_9\text{BrNO}_4$ $[\text{M} + \text{H}^+]$: 321.9709; found: 321.9701

(2E)-1-[4-(methylsulfanyl)phenyl]-3-(5-nitrofuran-2-yl)prop-2-en-1-one (LabMol-92) 17.

Brown solid; yield 24% (35 mg, 0.12 mmol); mp 160°C ; HPLC purity 99.15%. ^1H NMR (CDCl_3): $\delta = 8.00$ (d, 2H, $J = 8.0$ Hz), 7.76 (d, 1H, $J = 16.0$ Hz), 7.56 (d, 1H, $J = 16.0$ Hz),

1 7.39 (d, 1H, $J = 4.0$ Hz), 7.34 (d, 2H, $J = 8.0$ Hz), 6.84 (d, 1H, $J = 4.0$ Hz), 2.56 (s, 3H). ^{13}C
 2 NMR (CDCl_3): $\delta = 186.6, 152.8$ (2 C), 146.6, 132.9, 128.7 (2 C), 127.4, 124.7 (2 C), 124.5,
 3 115.9, 112.8, 14.3. IR (KBr): $\nu = 3117$ (m, $\nu(\text{C-H})$), 1658 (s; $\nu(\text{C=O})$), 1607 (s; $\nu(\text{C=C}_{\alpha\beta})$),
 4 1589, 1354 (s; $\nu(\text{Ar-NO}_2)$), 1394 (s; $\nu(\text{CH}_3)$). ESI (+)-MS (MeOH): $m/z = 290$ $[\text{M}+\text{H}]^+$, HR-
 5 MS (m/z) (ESI): calcd for $\text{C}_{14}\text{H}_{12}\text{NO}_4$ $[\text{M} + \text{H}^+]$: 258.0760; found: 258.0770

6 **(2E)-1-[4-(1H-imidazol-1-yl)phenyl]-3-(5-nitrothiophen-2-yl)prop-2-en-1-one (LabMol-84)**

7 **18.** Green solid; yield 55% (180 mg, 0.55 mmol); mp 223°C ; HPLC purity 98.99%. ^1H NMR
 8 ($[\text{D}_6]$ DMSO): $\delta = 9.80$ (s, 1H), 8.42 (d, 3H, $J = 8.0$ Hz), 8.17 (d, 1H, $J = 4.0$ Hz), 8.05 (d,
 9 1H, $J = 16.0$ Hz), 8.05 (d, 2H, $J = 8.0$ Hz), 7.95 (d, 1H, $J = 8.0$ Hz), 7.94 (d, 1H, $J = 16.0$
 10 Hz), 7.84 (d, 1H, $J = 4.0$ Hz). ^{13}C NMR ($[\text{D}_6]$ DMSO): $\delta = 187.2, 151.9, 146.4, 138.5, 137.1,$
 11 $135.5, 135.2, 131.5, 130.6$ (2 C), 130.6, 125.1, 122.0 (2 C), 121.7, 120.6. IR (KBr): $\nu = 1663$
 12 (s; $\nu(\text{C=O})$), 1605 (s; $\nu(\text{C=C}_{\alpha\beta})$), 1595, 1339 (s; $\nu(\text{Ar-NO}_2)$), 1284 (m; $\nu(\text{C-NAr})$). ESI (+)-
 13 MS (MeOH): $m/z = 326$ $[\text{M}+\text{H}]^+$. HR-MS (m/z) (ESI): calcd for $\text{C}_{16}\text{H}_{12}\text{N}_3\text{O}_3\text{S}$ $[\text{M}+\text{H}^+]$:
 14 326.0593; found: 326.0607.

15 **(2E)-1-(4-tert-butylphenyl)-3-(5-nitrothiophen-2-yl)prop-2-en-1-one (LabMol-86) 19.**

16 Green solid; yield 63% (99 mg, 0.31 mmol); mp 192°C ; HPLC purity 99.55%. ^1H NMR
 17 (CDCl_3): $\delta = 7.96$ (d, 2H, $J = 8.4$ Hz), 7.88 (d, 1H, $J = 4.4$ Hz), 7.80 (d, 1H, $J = 15.6$ Hz),
 18 7.55 (d, 2H, $J = 8.4$ Hz), 7.52 (d, 1H, $J = 15.6$ Hz), 7.27 (d, 1H, $J = 4.4$ Hz), 1.37 (s, 9H). ^{13}C
 19 NMR (CDCl_3): $\delta = 187.8, 157.1, 151.6, 146.1, 134.2, 134.09, 129.1, 128.7, 128.1$ (2 C),
 20 125.4 (2 C), 124.6, 34.8, 30.6 (3 C). IR (KBr): $\nu = 2962$ (s; $\nu(\text{C-H})$), 1657 (s; $\nu(\text{C=O})$), 1691
 21 (s; $\nu(\text{C=C}_{\alpha\beta})$), 1586, 1334 (s; $\nu(\text{Ar-NO}_2)$), 1366 (m; $\nu(\text{CH}_3)$). ESI (+)-MS (MeOH): $m/z =$
 22 316 $[\text{M}+\text{H}]^+$, HR-MS (m/z) (ESI): calcd for $\text{C}_{17}\text{H}_{18}\text{NO}_3\text{S}$ $[\text{M} + \text{H}^+]$: 316.1001; found:
 23 316.1006.

(2E)-1-(4-butylphenyl)-3-(5-nitrothiophen-2-yl)prop-2-en-1-one (LabMol-87) 20. Green

solid; yield 38% (61 mg, 0.19 mmol); mp 145° C; HPLC purity 99.76%. ¹H NMR (CDCl₃): δ = 7.95 (d, 2H, *J* = 8.0 Hz), 7.89 (d, 1H, *J* = 4.4 Hz), 7.80 (d, 1H, *J* = 15.6 Hz), 7.51 (d, 1H, *J* = 15.6 Hz), 7.34 (d, 2H, *J* = 8.0 Hz), 7.27 (d, 1H, *J* = 4.0 Hz), 2.71 (t, 2H, *J* = 8.0 Hz), 1.65 (q, 2H, *J* = 8.0 Hz), 1.38 (s, 2H, *J* = 8.0 Hz), 0.95 (t, 3H, *J* = 8.0 Hz) 3H). ¹³C NMR (CDCl₃): δ = 187.7, 151.5, 149.1, 146.1, 134.5, 134.0, 129.1, 128.7, 128.5 (2 C), 128.3 (2 C), 124.6, 35.3, 32.8, 21.9, 13.4. IR (KBr): ν = 2928 (s; ν(C-H)), 1657 (s; ν(C=O)), 1598 (s; ν(C=C_{αβ})), 1593, 1330 (s; ν(Ar-NO₂)), 1366 (m; ν(CH₃)), 816 (m; ν(CH₂)). ESI (+)-MS (MeOH): *m/z* = 316 [M+H]⁺, HR-MS (*m/z*) (ESI): calcd for C₁₇H₁₈NO₃S [M + H⁺]: 316.1001; found: 316.1005

(2E)-1-(4-cyclohexylphenyl)-3-(5-nitrothiophen-2-yl)prop-2-en-1-one (LabMol-88) 21.

Green solid; yield 64% (110 mg, 0.32 mmol); mp 182° C; HPLC purity 99.79%. ¹H NMR (CDCl₃): δ = 7.95 (d, 2H, *J* = 8.0 Hz), 7.88 (d, 1H, *J* = 4.0 Hz), 7.79 (d, 1H, *J* = 15.2 Hz), 7.52 (d, 1H, *J* = 15.2 Hz), 7.37 (d, 2H, *J* = 8.0 Hz), 7.27 (d, 1H, *J* = 4.0 Hz), 2.61 (s, 1H), 1.89 (s, 4H), 1.79 (s, 1H), 1.47 (s, 4H), 1.30 (s, 1H). ¹³C NMR (CDCl₃): δ = 187.7, 154.0, 151.5, 146.1, 134.6, 134.0, 129.1, 128.7, 128.4 (2 C), 126.9 (2 C), 124.7, 44.3, 33.6 (2 C), 26.3 (2 C), 25.6. IR (KBr): ν = 2926 (s; ν(C-H)), 1656 (s; ν(C=O)), 1606 (s; ν(C=C_{αβ})), 1589, 1334 (s; ν(Ar-NO₂)), 1427 (m; ν(CH₂)).

(2E)-1-[4-morpholin-4-yl]phenyl]-3-(nitrothiophen-2-yl)prop-2-en-1-one (LabMol-89) 22.

Yellow solid; yield 9% (17 mg, 0.04 mmol); mp 240° C; HPLC purity 98.62%. ¹H NMR (CDCl₃): δ = 7.99 (d, 2H, *J* = 9.2 Hz), 7.89 (d, 1H, *J* = 4.0 Hz), 7.79 (d, 1H, *J* = 15.2 Hz), 7.53 (d, 1H, *J* = 15.6 Hz), 7.25 (d, 1H, *J* = 4.4 Hz), 6.93 (d, 2H, *J* = 9.2 Hz), 3.88 (t, 4H, *J* = 4.0 Hz), 3.38 (t, 4H, *J* = 4.0 Hz). ¹³C NMR (CDCl₃): δ = 185.6, 154.1, 146.6 (2 C), 133.1, 130.4 (2 C), 128.7, 127.3, 124.8, 112.9 (2 C), 66.1 (2 C), 46.8 (2 C). IR (KBr): ν = 1648 (s;

1 $\nu(\text{C}=\text{O})$), 1604 (s; $\nu(\text{C}=\text{C}_{\alpha\beta})$), 1584, 1335 (s; $\nu(\text{Ar}-\text{NO}_2)$), 1428 (m; $\nu(\text{CH}_2)$), 1119 (w; $\nu(\text{C}-$
 2 O)). ESI (+)-MS (MeOH): $m/z = 345$ $[\text{M}+\text{H}]^+$.

3 **(2E)-1-[4-(methylsulfanyl)phenyl]-3-(5-nitrothiophen-2-yl)prop-2-en-1-one (LabMol-93)**

4 **23.** Green solid; yield 61% (189 mg, 0.61 mmol); mp 204° C; HPLC purity 99.21%. ^1H NMR
 5 (CDCl_3): $\delta = 7.95$ (d, 2H, $J = 8.0$ Hz), 7.89 (d, 1H, $J = 4.0$ Hz), 7.81 (d, 1H, $J = 16.0$ Hz),
 6 7.50 (d, 1H, $J = 16.0$ Hz), 7.34 (d, 2H, $J = 8.0$ Hz), 7.29 (d, 1H, $J = 4.0$ Hz), 2.57 (s, 3H). ^{13}C
 7 NMR (CDCl_3): $\delta = 186.9$, 146.6, 146.0, 134.2, 133.0, 129.2, 128.7, 128.5 (2 C), 124.7 (2 C),
 8 124.3, 14.3. IR (KBr): $\nu = 1654$ (s; $\nu(\text{C}=\text{O})$), 1604 (s; $\nu(\text{C}=\text{C}_{\alpha\beta})$), 1589, 1331 (s; $\nu(\text{Ar}-\text{NO}_2)$),
 9 1428 (m; $\nu(\text{CH}_3)$).

10 **(2E)-1-(4-methylphenyl)-3-(5-nitrothiophen-2-yl)prop-2-en-1-one (LabMol-95) 24.** Green

11 solid; yield 68% (186 mg, 0.68 mmol); mp 194° C; HPLC purity 99.4%. ^1H NMR (CDCl_3):
 12 7.94 (d, 2H, $J = 8.0$ Hz), 7.90 (d, 1H, $J = 4.0$ Hz), 7.81 (d, 1H, $J = 16.0$ Hz), 7.53 (d, 1H, $J =$
 13 16.0 Hz), 7.35 (d, 2H, $J = 8.0$ Hz), 7.28 (d, 1H, $J = 4.0$ Hz), 2.47 (s, 3H). ^{13}C NMR (CDCl_3):
 14 188.1, 146.4, 144.6, 134.7, 134.5, 129.6 (2C), 129.5, 129.1, 128.7 (2C), 125.0, 21.7. IR
 15 (KBr): $\nu = 3077$ (m; $\nu(\text{CH}_3)$), 1659 (s; $\nu(\text{C}=\text{O})$), 1609 (s; $\nu(\text{C}=\text{C}_{\alpha\beta})$), 1594, 1336 (s; $\nu(\text{Ar}-$
 16 $\text{NO}_2)$). ESI (+)-MS (MeOH): $m/z = 274$ $[\text{M}+\text{H}]^+$.

17 **(2E)-3-(5-chlorothiophen-2-yl)-1-[4-(1H-imidazol-1-yl)phenyl]prop-2-en-1-one**

18 **(LabMol-94) 25.** Green solid; yield 17% (54 mg, 0.17 mmol); mp 178° C; HPLC purity
 19 99.2%. ^1H NMR (CDCl_3): $\delta = 8.13$ (d, 2H, $J = 8.0$ Hz), 7.98 (s, 1H), 7.84 (d, 1H, $J = 16.0$
 20 Hz), 7.54 (d, 2H, $J = 8.0$ Hz), 7.38 (s, 1H), 7.24 (d, 2H, $J = 16.0$ Hz), 7.19 (s, 1H), 7.17 (d,
 21 1H, $J = 4.0$ Hz), 6.94 (d, 1H, $J = 4.0$ Hz). ^{13}C NMR (CDCl_3): $\delta = 188.6$, 140.5, 138.8, 137.1,
 22 136.5, 135.3, 134.0, 132.1, 131.1, 130.3 (2C), 127.7, 120.8 (2C), 119.9, 117.7. IR (KBr): $\nu =$
 23 1645 (s; $\nu(\text{C}=\text{O})$), 1608 (s; $\nu(\text{C}=\text{C}_{\alpha\beta})$), 810 (s; $\nu(\text{C}-\text{Cl})$). ESI (+)-MS (MeOH): $m/z = 315$
 24 $[\text{M}+\text{H}]^+$.

(2E)-3-(3-nitrophenyl)-1-[4-(piperidin-1-yl)phenyl]prop-2-en-1-one (LabMol-67) 26.

Yellow solid, yield 84% (84 mg, 0.25 mmol); mp 181°C; HPLC purity 99.97%. ¹H NMR (CDCl₃): 8.51 (s, 1H), 8.23 (d, 2H, *J* = 8.0 Hz), 8.01 (d, 2H, *J* = 8.0 Hz), 7.91 (d, 1H, *J* = 8.0 Hz), 7.80 (d, 1H, *J* = 16.0 Hz), 7.69 (d, 1H, *J* = 16.0 Hz), 7.60 (t, 1H, *J* = 8.0 Hz), 6.91 (d, 2H, *J* = 8.0 Hz), 3.43 (s, 4H), 1.69 (s, 6H). ¹³C NMR (CDCl₃): 186.5, 154.1, 148.3, 139.1, 136.8, 133.8, 130.6 (2 C), 129.5, 126.1, 124.4, 123.7, 121.6, 112.6 (2 C), 48.0 (2 C), 25.0 (2 C), 24.2. IR (KBr): ν = 2933 (m, ν (C-H)), 1651 (s; ν (C=O)), 1610 (s; ν (C=C _{$\alpha\beta$})), 1588, 1349 (s; ν (Ar-NO₂)), 1227 (s; ν (C-N)). ESI (+)-MS (MeOH): *m/z* = 337 [M+H]⁺

(2E)-3-[4-(dimethylamino)phenyl]-1-(4-phenylphenyl)prop-2-en-1-one (LabMol-69) 27.

Yellow solid; yield 53% (143 mg, 0.43 mmol); mp 164°C; HPLC purity 99.36%. ¹H NMR (CDCl₃): 8.07 (d, 2H, *J* = 4.0 Hz), 7.81 (s, 1H), 7.69 (d, 2H, *J* = 4.0 Hz), 7.63 (d, 2H, *J* = 4.0 Hz), 7.56 (d, 2H, *J* = 8.0 Hz), 7.45 (d, 2H, *J* = 8.0 Hz), 7.38 (d, 2H, *J* = 4.0 Hz), 6.68 (d, 2H, *J* = 4.0 Hz), 3.02 (s, 6H). ¹³C NMR (CDCl₃): 190.3, 152.3, 146.0, 145.1, 140.4, 138.0, 130.7 (2 C), 129.1 (3 C), 128.3 (2 C), 127.5 (2 C), 127.3 (2 C), 122.9, 112.1 (2 C), 40.3 (2 C). IR (KBr): ν = 1647 (s; ν (C=O)), 1603 (s; ν (C=C _{$\alpha\beta$})), 1228 (s; ν (C-N)). ESI (+)-MS (MeOH): *m/z* = 328 [M+H]⁺

(2E)-3-(4-methoxyphenyl)-1-(4-phenylphenyl)prop-2-en-1-one (LabMol-70) 28.

Yellow solid; yield 25% (79 mg, 0.25 mmol); mp 152°C; HPLC purity 100.00%. ¹H NMR (CDCl₃): 7.81 (d, 1H, *J* = 15.0 Hz), 8.09 (d, 2H, *J* = 10 Hz), 7.71 (d, 2H, *J* = 5.0 Hz), 7.64 (d, 2H, *J* = 10 Hz), 7.61 (d, 2H, *J* = 10 Hz), 7.45 (d, 1H, *J* = 15.0 Hz), 6.93 (d, 2H, *J* = 5.0 Hz), 3.84 (s, 3H). ¹³C NMR (CDCl₃): 190.2, 161.9, 145.5, 144.8, 140.2, 137.4, 130.5 (2 C), 129.3 (3 C), 128.4 (2 C), 127.9, 127.5 (2 C), 127.4 (2 C), 120.0, 114.7 (2 C), 55.6. IR (KBr): ν = 1647 (s; ν (C=O)), 1597 (s; ν (C=C _{$\alpha\beta$})), 1303, 1037 (s; ν (C-O)). ESI (+)-MS (MeOH): *m/z* = 315 [M+H]⁺

(2E)-3-(furan-2-yl)-1-[4-(methylsulfanyl)phenyl]prop-2-en-1-one (LabMol-71) 29.

Yellow solid; yield 19% (49 mg, 0.20 mmol); mp 114°C; HPLC purity 99.05%. ¹H NMR (CDCl₃): 7.95 (d, 2H, *J* = 6.8 Hz), 7.58 (d, 1H, *J* = 12.4 Hz), 7.51 (s, 1H), 7.43 (d, 1H, *J* = 12.4 Hz), 7.29 (d, 2H, *J* = 6.8 Hz), 6.70 (d, 1H, *J* = 2.4 Hz), 6.50 (q, 1H, *J* = 2.4 Hz), 2.52 (s, 3H). ¹³C NMR (CDCl₃): 188.6, 151.9, 145.7, 145.0, 134.6, 130.5, 129.0 (2 C), 125.2 (2 C), 119.2, 116.2, 112.8, 14.9. IR (KBr): ν = 1656 (s; ν (C=O)), 1596 (s; ν (C=C_{αβ})), 1549, 1476 (ArC=C), 1336 (s; ν (CH₃)), 1297, 1094 (s; ν (C-O)). ESI (+)-MS (MeOH): *m/z* = 245 [M+H]⁺.

(2E)-1-(3-iodophenyl)-3-(4-methoxyphenyl)prop-2-en-1-one (LabMol-76) 30. White

solid, yield 6% (22 mg, 0.06 mmol); mp 110°C; HPLC purity 99.64%. ¹H NMR (CDCl₃): δ = 8.32 (s, 1H), 7.96 (d, 1H, *J* = 8.0 Hz), 7.89 (d, 1H, *J* = 8.0 Hz), 7.79 (d, 1H, *J* = 15.6 Hz), 7.61 (d, 2H, *J* = 8.4 Hz), 7.33 (d, 1H, *J* = 15.6 Hz), 7.24 (t, 1H, *J* = 8.0 Hz), 6.95 (d, 2H, *J* = 8.0 Hz), 3.86 (s, 3H). ¹³C NMR (CDCl₃): δ = 188.5, 161.5, 145.1, 140.8, 139.9, 136.9, 130.0 (2 C), 129.8, 127.1, 126.9, 118.6, 114.1 (2 C), 94.0, 55.0. IR (KBr): ν = 1657 (s; ν (C=O)), 1600 (s; ν (C=C_{αβ})), 1559, 1510 (s, ν (ArC=C)), 1323 (s; ν (CH₃)). ESI (+)-MS (MeOH): *m/z* = 365 [M+H]⁺.

(2E)-3-(furan-2-yl)-1-[4-(piperidin-1-yl)phenyl]prop-2-en-1-one (LabMol-80) 31. Yellow

solid; yield 30% (86 mg, 0.30 mmol); mp 182° C; HPLC purity 99.32%. ¹H NMR (CDCl₃): δ = 8.00 (d, 2H, *J* = 8.8 Hz), 7.58 (d, 1H, *J* = 15.2 Hz), 7.54 (m, 1H), 7.50 (d, 1H, *J* = 15.2 Hz), 6.90 (d, 2H, *J* = 8.8 Hz), 6.67 (d, 1H, *J* = 3.2 Hz), 6.50 (dd, 1H, *J* = 3.2 Hz), 3.40 (s, 4H), 1.68 (s, 6H). ¹³C NMR (CDCl₃): δ = 186.8, 153.9, 151.7, 143.9, 130.3 (2 C), 128.6, 126.6, 119.2, 114.6, 112.9 (2 C), 112.0, 48.1 (2 C), 24.9 (2 C), 23.9. IR (KBr): ν = 2941 (m; ν (C-H), 1648 (s; ν (C=O)), 1604 (s; ν (C=C_{αβ})), 1597, 1559 (s, ν (ArC=C)), 1390 (s; ν (C-N)). ESI (+)-MS (MeOH): *m/z* = 282 [M+H]⁺.

(2E)-1-(3-bromophenyl)-3-(4-methoxyphenyl)prop-2-en-1-one (LabMol-83) 32. Brown

solid; yield 41% (130 mg, 0.41 mmol); mp 90°C; HPLC purity 99.66%. ¹H NMR (CDCl₃): δ = 8.13 (s, 1H), 7.93 (d, 1H, *J* = 8.0 Hz), 7.80 (d, 1H, *J* = 15.6 Hz), 7.70 (d, 1H, *J* = 8.0 Hz), 7.62 (d, 2H, *J* = 8.0 Hz), 7.39 (d, 1H, *J* = 8.0 Hz), 7.35 (d, 1H, *J* = 15.6 Hz), 6.95 (d, 2H, *J* = 8.0 Hz), 3.87 (s, 3H). ¹³C NMR (CDCl₃): δ = 188.6, 161.5, 145.1, 139.9, 134.9, 131.0, 130.0 (2 C), 129.7, 126.9, 126.5, 122.5, 118.6, 114.1 (2 C), 55.0. IR (KBr): ν = 1662 (s; ν(C=O)), 1594 (s; ν(C=C_{αβ})), 1570, 1513 (s, ν(ArC=C)), 1260, 1042 (s; ν(C-O)), 556 (m, ν(C-Br)).

(2E)-1-(4-tert-butylphenyl)-3-(1H-pyrrol-2-yl)prop-2-en-1-one (LabMol-85) 33. White

solid; yield 7% (20 mg, 0.07 mmol); mp 158° C; HPLC purity 99.81%. ¹H NMR (CDCl₃): δ = 9.07 (s, 1H), 7.95 (d, 2H, *J* = 8.4 Hz), 7.77 (d, 1H, *J* = 15.6 Hz), 7.50 (d, 2H, *J* = 8.4 Hz), 7.19 (d, 1H, *J* = 15.6 Hz), 7.00 (s, 1H), 6.72 (s, 1H), 6.34 (s, 1H), 1.36 (s, 9H). ¹³C NMR (CDCl₃): δ = 189.6, 155.7, 135.5, 133.9, 128.9, 127.8 (2 C), 125.1 (2 C), 122.6, 115.4, 114.6, 111.0, 34.6, 30.7 (3 C). ESI (+)-MS (MeOH): *m/z* = 254 [M+H]⁺.

(2E)-3-(4-nitrophenyl)-1-[4-piperidin-1-yl]phenylprop-2-en-1-one (LabMol-90) 34.

Yellow solid, yield 89% (300 mg, 0.89 mmol); mp 198°C; HPLC purity 99.50%. ¹H NMR (CDCl₃): δ = 8.25 (d, 2H, *J* = 8.0 Hz), 7.99 (d, 2H, *J* = 8.0 Hz), 7.78 (d, 1H, *J* = 16.0 Hz), 7.77 (d, 2H, *J* = 8.0 Hz), 7.68 (d, *J* = 16.0 Hz), 6.90 (d, 2H, *J* = 8.0 Hz), 3.41 (s, 4H), 1.69 (s, 6H). ¹³C NMR (CDCl₃): δ = 186.2, 154.1, 147.8, 141.3, 139.0, 130.6 (2 C), 130.0, 128.2 (2 C), 126.0, 125.6, 123.7 (2 C), 112.7 (2 C), 48.0 (2 C), 24.9 (2 C), 23.9. IR (KBr): ν = 2942 (m, ν(C-H)), 1655 (s; ν(C=O)), 1609 (s; ν(C=C_{αβ})), 1595, 1514 (s, ν(ArC=C)), 1593, 1336 (s, ν(Ar-NO₂)), 1196 (s; ν(C-N)), 556 (m, ν(C-Br)). ESI (+)-MS (MeOH): *m/z* = 337 [M+H]⁺.

(2E)-1-(4-tert-butylphenyl)-3-(furan-2-yl)prop-2-en-1-one (LabMol-91) 35. Yellow solid;

yield 7.8% (20 mg, 257 mmol); mp 84°C; HPLC purity 99.8%. ¹H NMR (CDCl₃): δ = 7.99 (d, 2H, *J* = 8.4 Hz), 7.60 (d, 1H, *J* = 15.2 Hz), 7.52 (d, 3H, *J* = 8.4 Hz), 7.48 (d, 1H, *J* = 15.2

Hz), 6.72 (s, 1H), 6.52 (s, 1H), 1.37 (s, 9H). ^{13}C NMR (CDCl_3): δ = 188.7, 156.1, 151.3, 144.3, 135.1, 129.9, 128.0 (2 C), 125.1 (2 C), 119.0, 115.5, 112.2, 34.7, 30.7 (3 C). IR (KBr): ν = 2962 (m, $\nu(\text{C-H})$), 1655 (s; $\nu(\text{C=O})$), 1605 (s; $\nu(\text{C=C}_{\alpha\beta})$), 1285 (s, $\nu(\text{C-O})$). ESI (+)-MS (MeOH): m/z = 255 $[\text{M}+\text{H}]^+$.

Biological Evaluation

Anti-TB activity. MICs against *M. tb.* H37Rv (ATCC 27294) as well as the rifampin (rRMP, ATCC 35838) and isoniazid (rINH, ATCC 35822) mono-resistant strains under normoxic, replicating conditions were determined using the Microplate Assay Blue Alamar (MABA) as previously described [91–93]. Briefly, cultures were incubated in 200 μL Middlebrook 7H12 medium together with test compound in 96-well plates for 7d and 37° C. Resazurin and Tween 80 were added and incubation continued for 24h at 37° C. Fluorescence was determined at excitation/emission wavelengths of 530/590 nm, respectively. The MIC was defined as the lowest concentration effecting a reduction in fluorescence of 90% relative to controls.⁶¹ MICs against *M. tb.* H37Rv under hypoxic, non-replicating conditions were determined using the Low Oxygen Recovery Assay as previously described [82,93] except that the luxABCDE reporter[95] was used instead of the luxAB reporter gene. The MIC was defined as the lowest concentration of compound which reduced luminescence by 90% after 10 days exposure to compound under hypoxic conditions followed by 28 hours of normoxic recovery and comparison to untreated controls.

Cytotoxicity in mammalian cells. Vero cells (ATCC CRL-1586) were cultured in 10% Fetal Bovine Serum (FBS) in Eagle minimum essential medium plus penicillin and streptomycin. Cells were prepared and washed in HBSS (1x pH = 7.4) and Trypsin-EDTA 0.25%, and then morphology was verified by microscopy. After adjusting the density to $3\text{--}5 \times 10^5$ cells/mL in MEM media, 100 μL of the cell suspension were incubated with test compounds at 37° C for

72 hours; visual inspection was performed each 24 hours. Then, 20 μ L of 0.6 mM resazurin were added into each well and incubated for 4 hours. The fluorescence was determined by excitation/emission wavelengths of 530/590 nm. The concentration of test compound effecting a reduction in fluorescence of 50% relative to untreated cells was calculated as the IC₅₀.

Spectrum of activity. *Mycobacterium abscessus* (ATCC 19977), *M. chelonae* (ATCC 35752), *M. marinum* (ATCC 927), *M. avium* (ATCC 15769), *M. kansasii* (ATCC 12478), and *M. bovis* (ATCC 35734) were cultured in Middlebrook 7H9 Broth with 0.2% (v/v) glycerol, 0.05% Tween 80, and 10% (v/v) albumin-dextrose-catalase (BBL™ OADC Enrichment, Cat. N°. 212352). *M. smegmatis* (ATCC MC2155) was cultured in 7H12 medium. *Escherichia coli* (ATCC 25922) and *Staphylococcus aureus* (ATCC 29213) were cultured in cation-adjusted Mueller Hinton (CAMH) broth and *Candida albicans* (ATCC 90028) in RPMI media until an absorbance at 570 nm of 0.2-0.5 was achieved. Cultures were diluted 1:5000 to 1:10,000 into fresh media in 96-well plates and incubated at 37° C with test compounds. Incubation times were 3 days for *M. smegmatis*, 3-7 days for other mycobacteria, 36-48 hours for *C. albicans* and 16-20 hours for *S. aureus* and *E. coli*. The MIC for *C. albicans*, *S. aureus* and *E. coli* was defined as the lowest concentration effecting a reduction of $\geq 90\%$ in A₅₇₀ relative to untreated cultures. The MABA MICs for mycobacteria are defined as described above.

ASSOCIATED CONTENT

Supporting Information. More computational details regarding molecular fingerprints calculation and QSAR model development are available in the Supporting Information, as well as additional tables of results and structural characterization for all synthesized compounds. This material is available free of charge via the Internet at <http://ejmedch>.

AUTHOR INFORMATION

Corresponding Authors

*LabMol, Laboratory for Molecular Modeling and Drug Design, Faculdade de Farmácia, Universidade Federal de Goiás, Rua 240, Qd.87, Setor Leste Universitário, Goiânia – GO 74605-170, Brazil. Tel: + 55 62 3209-6451; Fax: +55 62 3209-6037; E-mail: carolina@ufg.br

* Institute for Tuberculosis Research, University of Illinois at Chicago, 833 South Wood Street, Chicago, Illinois 60612, United States. Tel: 312-355-1715; E-mail: sgf@uic.edu

Funding Sources

M.N.G. was supported by a sandwich fellowship from the Coordination for the Improvement of Higher Education Personnel (CAPES-PDSE) during his stay in ITR-UIC. M.N.G. is also supported by a Ph.D. fellowship from the State of Goiás Research Foundation (FAPEG). This work has been funded by the National Counsel of Technological and Scientific Development (CNPq), the State of Goiás Research Foundation (FAPEG). C.H.A. is CNPq productivity fellow. The funders had no role in study design, data collection and analysis, decision to publish, or preparation of the manuscript.

Notes

The authors declare no competing financial interest.

ACKNOWLEDGMENT

The authors would like to thank Brazilian funding agencies, CNPq, CAPES and FAPEG for financial support and fellowships. We are grateful to OpenEye Scientific Software, Inc. and ChemAxon for providing academic license of their software.

ABBREVIATIONS

TB, tuberculosis; *M. tb.*, *Mycobacterium tuberculosis*; WHO, World Health Organization; DOTS, Directly Observed Therapy Short-course; RMP, rifampin; INH, isoniazid; PZA, pyrazinamide; EMB, ethambutol; DS-TB, drug sensitive TB; MDR-TB, multidrug-resistance; XDR-TB, extensively drug-resistance; STOP-TB, STOP tuberculosis strategy; CADD, computer assisted drug design; QSAR, Quantitative Structure Activity Relationship; MMPA, Matched Molecular Pairs of Analysis; SAR, Structure Activity Relationship; MACCS, Molecular ACCess System keys; SVM, Support Vector Machine; RF, Random Forest; CCR, correct classification rate; Se, sensitivity; Sp, Specificity; NMR, Nuclear Magnetic Resonance; MS, Mass Spectrometry; HPLC, High-Performance Liquid Chromatography; MABA, microplate alamar blue assay; LORA, low oxygen recovery assay; MIC, minimum inhibitory concentration; SI, selectivity index; NTM, non-tuberculosis mycobacterias; AD, applicability domain; DMSO, dimethylsulfoxide; ATCC, American Type Culture Collection; CAMH, Mueller Hinton Media; RPMI, Roswell Park Memorial Institute; HBSS, Hank's Balanced Salt Solution; rRMP, resistant isogenic strain rifampin; rINH, resistant isogenic isoniazid.

REFERENCES

- [1] B.D. Palmer, H.S. Sutherland, A. Blaser, I. Kmentova, S.G. Franzblau, B. Wan, Y. Wang, Z. Ma, W. a. Denny, A.M. Thompson, Synthesis and Structure-Activity Relationships for Extended Side Chain Analogues of the Antitubercular Drug (6 S)-2-Nitro-6-[[4-(trifluoromethoxy)benzyl]oxy]-6,7-dihydro-5 H -imidazo[2,1-b][1,3]oxazine (PA-824), J. Med. Chem. 58 (2015) 3036–3059. doi:10.1021/jm501608q.
- [2] F. Martins, S. Santos, C. Ventura, R. Elvas-Leitão, L. Santos, S. Vitorino, M. Reis, V.

Miranda, H.F. Correia, J. Aires-de-Sousa, V. Kovalishyn, D. a. R.S. Latino, J. Ramos, M. Viveiros, Design, synthesis and biological evaluation of novel isoniazid derivatives with potent antitubercular activity, *Eur. J. Med. Chem.* 81 (2014) 119–138. doi:10.1016/j.ejmech.2014.04.077.

[3] WHO, Global Tuberculosis 2015, (2015).

[4] J. Tang, W.-C. Yam, Z. Chen, Mycobacterium tuberculosis infection and vaccine development, *Tuberculosis*. 98 (2016) 30–41. doi:10.1016/j.tube.2016.02.005.

[5] S.T. Cole, G. Riccardi, New tuberculosis drugs on the horizon, *Curr. Opin. Microbiol.* 14 (2011) 570–576. doi:10.1016/j.mib.2011.07.022.

[6] C.H. Andrade, L.D.B. Salum, M.S. Castilho, K.F.M. Pasqualoto, E.I. Ferreira, A.D. Andricopulo, Fragment-based and classical quantitative structure-activity relationships for a series of hydrazides as antituberculosis agents., *Mol. Divers.* 12 (2008) 47–59. doi:10.1007/s11030-008-9074-z.

[7] A. Lilienkampf, M. Pieroni, B. Wan, Y. Wang, S.G. Franzblau, A.P. Kozikowski, Rational design of 5-phenyl-3-isoxazolecarboxylic acid ethyl esters as growth inhibitors of Mycobacterium tuberculosis. a potent and selective series for further drug development., *J. Med. Chem.* 53 (2010) 678–88. doi:10.1021/jm901273n.

[8] M. Pieroni, A. Lilienkampf, W. Baojie, W. Yuehong, S.G. Franzblau, A.P. Kozikowski, Synthesis, biological evaluation, and structure-activity relationships for 5-[(E)-2-arylethenyl]-3-isoxazolecarboxylic acid alkyl ester derivatives as valuable antitubercular chemotypes, *J. Med. Chem.* 52 (2009) 6287–6296. doi:10.1021/jm900513a.

[9] WHO, The Stop TB Strategy, (2015).

- [10] TBALLIANCE, TB ALLIANCE Putting science to work for a faster TB cure, [Www.tballiance.org](http://www.tballiance.org). (2015).
- [11] R. Mahajan, Bedaquiline: First FDA-approved tuberculosis drug in 40 years, *Int. J. Appl. Basic Med. Res.* 2 (2013) 124–128. doi:10.4103/2229.
- [12] a S. Xavier, M. Lakshmanan, Delamanid: A new armor in combating drug-resistant tuberculosis, *J Pharmacol Pharmacother.* 5 (2014) 222–224. doi:10.4103/0976-500X.136121.
- [13] D. Dobchev, G. Pillai, M. Karelson, In silico machine learning methods in drug development, *Curr. Top. Med. Chem.* 14 (2014) 1913–1922. doi:10.2174/1568026614666140929124203.
- [14] C.M. Song, S.J. Lim, J.C. Tong, Recent advances in computer-aided drug design, *Brief. Bioinform.* 10 (2009) 579–591. doi:10.1093/bib/bbp023.
- [15] C.C. Melo-Filho, R.C. Braga, C.H. Andrade, 3D-QSAR Approaches in Drug Design: Perspectives to Generate Reliable CoMFA Models., *Curr. Comput. Aided. Drug Des.* 10 (2014) 148–59. <http://www.ncbi.nlm.nih.gov/pubmed/24724896> (accessed September 1, 2014).
- [16] R.C. Braga, V.M. Alves, A.C. Silva, L.M. Liao, C.H. Andrade, Virtual Screening Strategies in Medicinal Chemistry: The state of the art and current challenges, *Curr. Top. Med. Chem.* 14 (2014) 1899–1912. doi:10.2174/1568026614666140929120749.
- [17] M.G. Albuquerque, M.A. de Brito, R.B. de Alencastro, O.A.C. Antunes, H.C. Castro, C.R. Rodrigues, Multidimensional-QSAR: Beyond the third-dimension in drug design., in: C.A. Taft, C.H.T.P. Silva (Eds.), *Curr. Methods Med. Chem. Biol. Phys.*, Research signpost, Kerala, 2007: pp. 91–100.

- [18] R.V.C. Guido, G. Oliva, A.D. Andricopulo, Modern drug discovery technologies: opportunities and challenges in lead discovery., Comb. Chem. High Throughput Screen. 14 (2011) 830–839. <http://www.ncbi.nlm.nih.gov/pubmed/21843147> (accessed May 8, 2013).
- [19] V. Kovalishyn, J. Aires-de-Sousa, C. Ventura, R. Elvas Leita, F. Martins, QSAR modeling of antitubercular activity of diverse organic compounds, Chemom. Intell. Lab. Syst. 107 (2011) 69–74. doi:10.1016/j.chemolab.2011.01.011.
- [20] G. Klopman, D. Fercu, J. Jacob, Computer-aided study of the relationship between structure and antituberculosis activity of a series of isoniazid derivatives, Chem. Phys. 204 (1996) 181–193. doi:10.1016/0301-0104(95)00415-7.
- [21] R. Mehra, C. Rani, P. Mahajan, R.A. Vishwakarma, I.A. Khan, A. Nargotra, Computationally Guided Identification of Novel *Mycobacterium tuberculosis* GlmU Inhibitory Leads, Their Optimization, and in Vitro Validation, ACS Comb. Sci. 18 (2016) 100–116. doi:10.1021/acscombsci.5b00019.
- [22] R.C. Khunt, V.M. Khedkar, R.S. Chawda, N.A. Chauhan, A.R. Parikh, E.C. Coutinho, Synthesis, antitubercular evaluation and 3D-QSAR study of N-phenyl-3-(4-fluorophenyl)-4-substituted pyrazole derivatives, Bioorg. Med. Chem. Lett. 22 (2012) 666–678. doi:10.1016/j.bmcl.2011.10.059.
- [23] A. Nayyar, A. Malde, R. Jain, E. Coutinho, 3D-QSAR study of ring-substituted quinoline class of anti-tuberculosis agents, Bioorganic Med. Chem. 14 (2006) 847–856. doi:10.1016/j.bmc.2005.09.018.
- [24] V. Virsodia, R.R.S. Pissurlenkar, D. Manvar, C. Dholakia, P. Adlakha, A. Shah, E.C. Coutinho, Synthesis, screening for antitubercular activity and 3D-QSAR studies of substituted N-phenyl-6-methyl-2-oxo-4-phenyl-1,2,3,4-tetrahydro-pyrimidine-5-

- carboxamides, *Eur. J. Med. Chem.* 43 (2008) 2103–2115.
- [25] R. Ragno, F. Ballante, Pharmacophore Assessment Through 3-D QSAR: evaluation of the predictive ability on new derivatives by the application on a serie of antitubercular agents., *J. Chem. Inf. Model.* (2013). doi:10.1021/ci400132q.
- [26] R.A. Gupta, S.G. Kaskhedikar, Synthesis, antitubercular activity, and QSAR analysis of substituted nitroaryl analogs: Chalcone, pyrazole, isoxazole, and pyrimidines, *Med. Chem. Res.* 22 (2013) 3863–3880. doi:10.1007/s00044-012-0385-3.
- [27] C. Ventura, D.A.R.S. Latino, F. Martins, Comparison of multiple linear regressions and neural networks based QSAR models for the design of new antitubercular compounds, *Eur. J. Med. Chem.* 70 (2013) 831–845. doi:10.1016/j.ejmech.2013.10.029.
- [28] S.D. Joshi, U.A. More, T.M. Aminabhavi, A.M. Badiger, Two- and three-dimensional QSAR studies on a set of antimycobacterial pyrroles: CoMFA, Topomer CoMFA, and HQSAR, *Med. Chem. Res.* 23 (2014) 107–126. doi:10.1007/s00044-013-0607-3.
- [29] R.C. Khunt, V.M. Khedkar, E.C. Coutinho, Synthesis and 3D-QSAR analysis of 2-chloroquinoline derivatives as H 37 RV MTB inhibitors, *Chem. Biol. Drug Des.* 82 (2013) 669–684. doi:10.1111/cbdd.12178.
- [30] G. Stavrakov, V. Valcheva, I. Philipova, I. Doytchinova, Design of novel camphane-based derivatives with antimycobacterial activity, *J. Mol. Graph. Model.* 51 (2014) 7–12. doi:10.1016/j.jmgm.2014.04.008.
- [31] V. Frecer, P. Seneci, S. Miertus, Computer-assisted combinatorial design of bicyclic thymidine analogs as inhibitors of Mycobacterium tuberculosis thymidine monophosphate kinase, *J. Comput. Aided. Mol. Des.* 25 (2011) 31–49. doi:10.1007/s10822-010-9399-4.

- [32] A. Kumar, M.I. Siddiqi, CoMFA based de novo design of pyrrolidine carboxamides as inhibitors of enoyl acyl carrier protein reductase from *Mycobacterium tuberculosis*., J. Mol. Model. 14 (2008) 923–35. doi:10.1007/s00894-008-0326-8.
- [33] S. Syam, S.I. Abdelwahab, M.A. Al-Mamary, S. Mohan, Synthesis of chalcones with anticancer activities., Molecules. 17 (2012) 6179–95. doi:10.3390/molecules17066179.
- [34] N. Aoki, M. Muko, E. Ohta, S. Ohta, C-geranylated chalcones from the stems of *Angelica keiskei* with superoxide-scavenging activity, J. Nat. Prod. 71 (2008) 1308–1310. doi:10.1021/np800187f.
- [35] Y.H. Chen, W.H. Wang, Y.H. Wang, Z.Y. Lin, C.C. Wen, C.Y. Chern, Evaluation of the anti-inflammatory effect of chalcone and chalcone analogues in a Zebrafish model, Molecules. 18 (2013) 2052–2060. doi:10.3390/molecules18022052.
- [36] D.K. Mahapatra, S.K. Bharti, V. Asati, Anti-cancer chalcones: Structural and molecular target perspectives., Eur. J. Med. Chem. 98 (2015) 69–114. doi:10.1016/j.ejmech.2015.05.004.
- [37] S.U.F. Rizvi, H.L. Siddiqui, M. Johns, M. Detorio, R.F. Schinazi, Anti-HIV-1 and cytotoxicity studies of piperidyl-thienyl chalcones and their 2-pyrazoline derivatives, Med. Chem. Res. 21 (2012) 3741–3749. doi:10.1007/s00044-011-9912-x.
- [38] R.H. Hans, E.M. Guantai, C. Lategan, P.J. Smith, B. Wan, S.G. Franzblau, J. Gut, P.J. Rosenthal, K. Chibale, Synthesis, antimalarial and antitubercular activity of acetylenic chalcones., Bioorg. Med. Chem. Lett. 20 (2010) 942–4. doi:10.1016/j.bmcl.2009.12.062.
- [39] M. Chen, L. Zhai, S.B. Christensen, T.G. Theander, A. Kharazmi, Inhibition of Fumarate Reductase in *Leishmania major* and *L. donovani* by Chalcones, Antimicrob. Agents Chemother. 45 (2001) 2023–2029.

- [40] M. Ouattara, D. Sissouma, M.W. Koné, E. Hervé, S.A. Touré, L. Ouattara, Synthesis and anthelmintic activity of some hybrid Benzimidazolyl-chalcone derivatives, 10 (2011) 767–775.
- [41] S.N. López, M. V Castelli, S. a Zacchino, J.N. Domínguez, G. Lobo, J. Charris-Charris, J.C. Cortés, J.C. Ribas, C. Devia, a M. Rodríguez, R.D. Enriz, In vitro antifungal evaluation and structure-activity relationships of a new series of chalcone derivatives and synthetic analogues, with inhibitory properties against polymers of the fungal cell wall., *Bioorg. Med. Chem.* 9 (2001) 1999–2013.
- [42] G. Avila-Villarreal, O. Hernández-Abreu, S. Hidalgo-Figueroa, G. Navarrete-Vázquez, F. Escalante-Erosa, L.M. Peña-Rodríguez, R. Villalobos-Molina, S. Estrada-Soto, Antihypertensive and vasorelaxant effects of dihydropinochalcone-A isolated from *Lonchocarpus xuul* Lundell by NO production: Computational and ex vivo approaches., *Phytomedicine*. (2013). doi:10.1016/j.phymed.2013.06.011.
- [43] T. Yamamoto, M. Yoshimura, F. Yamaguchi, T. Kouchi, R. Tsuji, M. Saito, A. Obata, M. Kikuchi, Anti-allergic activity of naringenin chalcone from a tomato skin extract., *Biosci. Biotechnol. Biochem.* 68 (2004) 1706–1711. doi:10.1271/bbb.68.1706.
- [44] H. Jamal, W.H. Ansari, S.J. Rizvi, Evaluation of chalcones - A flavonoid subclass, for, their anxiolytic effects in rats using elevated plus maze and open field behaviour tests, *Fundam. Clin. Pharmacol.* 22 (2008) 673–681. doi:10.1111/j.1472-8206.2008.00639.x.
- [45] K.W. Lam, R. Uddin, C.Y. Liew, C.L. Tham, D. a. Israf, A. Syahida, M.B.A. Rahman, Z. Ul-Haq, N.H. Lajis, Synthesis and QSAR analysis of chalcone derivatives as nitric oxide inhibitory agent, *Med. Chem. Res.* 21 (2011) 1953–1966. doi:10.1007/s00044-011-9706-1.
- [46] Y. Sato, J.-X. He, H. Nagai, T. Tani, T. Akao, Isoliquiritigenin, one of the

- antispasmodic principles of *Glycyrrhiza uralensis* roots, acts in the lower part of intestine., *Biol. Pharm. Bull.* 30 (2007) 145–149. doi:10.1248/bpb.30.145.
- [47] D. Batovska, S. Parushev, B. Stamboliyska, I. Tsvetkova, M. Ninova, H. Najdenski, Examination of growth inhibitory properties of synthetic chalcones for which antibacterial activity was predicted., *Eur. J. Med. Chem.* 44 (2009) 2211–8. doi:10.1016/j.ejmech.2008.05.010.
- [48] Z. Nowakowska, A review of anti-infective and anti-inflammatory chalcones., *Eur. J. Med. Chem.* 42 (2007) 125–37. doi:10.1016/j.ejmech.2006.09.019.
- [49] L.D. Chiaradia, A. Mascarello, M. Purificação, J. Vernal, M.N.S. Cordeiro, M.E. Zenteno, A. Villarino, R.J. Nunes, R.A. Yunes, H. Terenzi, Synthetic chalcones as efficient inhibitors of *Mycobacterium tuberculosis* protein tyrosine phosphatase PtpA., *Bioorg. Med. Chem. Lett.* 18 (2008) 6227–30. doi:10.1016/j.bmcl.2008.09.105.
- [50] A. García, V. Bocanegra-García, J.P. Palma-Nicolás, G. Rivera, Recent advances in antitubercular natural products., *Eur. J. Med. Chem.* 49C (2012) 1–23. doi:10.1016/j.ejmech.2011.12.029.
- [51] PubChem, PubChem Bioassay, (n.d.).
- [52] ChEMBL, ChEMBL-European Bioinformatics Institute, (2014).
- [53] Scifinder, SciFinder-Chemical Abstracts Service, (2014).
- [54] D. Fourches, E.N. Muratov, A. Tropsha, Trust, But Verify II: A Practical Guide to Chemogenomics Data Curation, *J. Chem. Inf. Model.* (2016) DOI:10.1021/acs.jcim.6b00129. doi:10.1021/acs.jcim.6b00129.
- [55] D. Fourches, E. Muratov, A. Tropsha, Trust, but verify: on the importance of chemical structure curation in cheminformatics and QSAR modeling research., *J. Chem. Inf.*

- Model. 50 (2010) 1189–204. doi:10.1021/ci100176x.
- [56] D. Fourches, E. Muratov, A. Tropsha, Curation of chemogenomics data., *Nat. Chem. Biol.* 11 (2015) 535. doi:10.1038/nchembio.1881.
- [57] A. Varnek, D. Fourches, D. Horvath, O. Klimchuk, C. Gaudin, P. Vayer, V. Solov'ev, F. Hoonakker, I. V Tetko, G. Marcou, ISIDA - Platform for Virtual Screening Based on Fragment and Pharmacophoric Descriptors, *Curr. Comput. Aided. Drug Des.* 4 (2008) 191–198. doi:10.2174/157340908785747465.
- [58] V.E. Kuz'min, a G. Artemenko, E.N. Muratov, Hierarchical QSAR technology based on the Simplex representation of molecular structure., *J. Comput. Aided. Mol. Des.* 22 (2008) 403–421. doi:10.1007/s10822-008-9179-6.
- [59] P.W. Kenny, J. Sadowski, Structure Modification in Chemical Databases, in: *Chemoinformatics Drug Discov.*, Wiley-VCH Verlag GmbH & Co. KGaA, 2005: pp. 271–285. doi:10.1002/3527603743.ch11.
- [60] A.G. Leach, H.D. Jones, D.A. Cosgrove, P.W. Kenny, L. Ruston, P. MacFaul, J.M. Wood, N. Colclough, B. Law, Matched Molecular Pairs as a Guide in the Optimization of Pharmaceutical Properties; a Study of Aqueous Solubility, Plasma Protein Binding and Oral Exposure, *J. Med. Chem.* 49 (2006) 6672–6682. doi:10.1021/jm0605233.
- [61] MACCS structural keys. 2013, Accelrys, San Diego, CA., (n.d.).
- [62] J.D. Holliday, S.S. Ranade, P. Willett, A Fast Algorithm For Selecting Sets Of Dissimilar Molecules From Large Chemical Databases, *Quant. Struct. Relationships.* 14 (1995) 501–506. doi:10.1002/qsar.19950140602.
- [63] L. Wang, A. Evers, P. Monecke, T. Naumann, Ligand based lead generation - considering chemical accessibility in rescaffolding approaches via BROOD, *J.*

- Cheminform. 4 (2012) O20. doi:10.1186/1758-2946-4-S1-O20.
- [64] M. Wirth, V. Zoete, O. Michielin, W.H.B. Sauer, SwissBioisostere: A database of molecular replacements for ligand design, *Nucleic Acids Res.* 41 (2013) 1–7. doi:10.1093/nar/gks1059.
- [65] N.M. O’Boyle, C. Morley, G.R. Hutchison, Pybel: a Python wrapper for the OpenBabel cheminformatics toolkit., *Chem. Cent. J.* 2 (2008) 5. doi:10.1186/1752-153X-2-5.
- [66] R.E. Carhart, D.H. Smith, R. Venkataraghavan, Atom Pairs as Molecular Features in Structure-Activity Studies : Definition and Applications, 13 (1985) 8–11.
- [67] S. Riniker, G. a Landrum, Open-source platform to benchmark fingerprints for ligand-based virtual screening., *J. Cheminform.* 5 (2013) 26. doi:10.1186/1758-2946-5-26.
- [68] D. Rogers, M. Hahn, Extended-connectivity fingerprints., *J. Chem. Inf. Model.* 50 (2010) 742–54.
- [69] H.L. Morgan, The Generation of a Unique Machine Description for Chemical Structures-A Technique Developed at Chemical Abstracts Service., *J. Chem. Doc.* 5 (1965) 107–113. doi:10.1021/c160017a018.
- [70] P. Gedeck, B. Rohde, C. Bartels, Article QSAR – How Good Is It in Practice ? Comparison of Descriptor Sets on an Unbiased Cross Section of Corporate Data Sets QSAR - How Good Is It in Practice ? Comparison of Descriptor Sets on an Unbiased Cross Section of Corporate Data Sets, (2006) 1924–1936. doi:10.1021/ci050413p.
- [71] V. Vapnik, *The Nature of Statistical Learning Theory*, 2nd ed., Springer, New York, 2000.
- [72] A. Natekin, A. Knoll, Gradient boosting machines, a tutorial., *Front. Neurorobot.* 7

- (2013) 21. doi:10.3389/fnbot.2013.00021.
- [73] L. Breiman, Random Forest, Mach. Learn. (2001) 1–33. doi:10.1023/A:1010933404324.
- [74] D.F. Veber, S.R. Johnson, H.-Y. Cheng, B.R. Smith, K.W. Ward, K.D. Kopple, Molecular properties that influence the oral bioavailability of drug candidates., J. Med. Chem. 45 (2002) 2615–23. <http://www.ncbi.nlm.nih.gov/pubmed/12036371>.
- [75] C.A. Lipinski, F. Lombardo, B.W. Dominy, P.J. Feeney, Experimental and computational approaches to estimate solubility and permeability in drug discovery and development settings, Adv. Drug Deliv. Rev. 23 (1997) 3–25. doi:10.1016/S0169-409X(96)00423-1.
- [76] J. Baell, M.A. Walters, Chemistry: Chemical con artists foil drug discovery, Nature. 513 (2014) 481–483. doi:10.1038/513481a.
- [77] J.B. Baell, G. a. Holloway, New substructure filters for removal of pan assay interference compounds (PAINS) from screening libraries and for their exclusion in bioassays, J. Med. Chem. 53 (2010) 2719–2740. doi:10.1021/jm901137j.
- [78] S. Nasir Abbas Bukhari, M. Jasamai, I. Jantan, W. Ahmad, Review of Methods and Various Catalysts Used for Chalcone Synthesis, Mini. Rev. Org. Chem. 10 (2013) 73–83. doi:10.2174/1570193X11310010006.
- [79] N.R. Tawari, R. Bairwa, M.K. Ray, M.G.R. Rajan, M.S. Degani, Design, synthesis, and biological evaluation of 4-(5-nitrofuran-2-yl)prop-2-en-1-one derivatives as potent antitubercular agents., Bioorg. Med. Chem. Lett. 20 (2010) 6175–8. doi:10.1016/j.bmcl.2010.08.127.
- [80] A. Cisak, Rzeszowska-Modzelewska, E. Brzezinska, Reactivity of 5-nitro-2-

- furaldehyde in alkaline and acidic solutions, (2001) 427–434.
- [81] L. a. Collins, Franzblau, Scott G., Microplate Almar Blue Assay versus BACTEC 460 System for High-throughput Screening of Compounds against Mycobacterium tuberculosis and Mycobacterium avium, *Antimicrob. Agents Chemother.* 41 (1997) 1004–1009.
- [82] S.H. Cho, S. Warit, B. Wan, C.H. Hwang, G.F. Pauli, S.G. Franzblau, Low-oxygen-recovery assay for high-throughput screening of compounds against nonreplicating Mycobacterium tuberculosis., *Antimicrob. Agents Chemother.* 51 (2007) 1380–5. doi:10.1128/AAC.00055-06.
- [83] K. Katsuno, J.N. Burrows, K. Duncan, R.H. van Huijsduijnen, T. Kaneko, K. Kita, C.E. Mowbray, D. Schmatz, P. Warner, B.T. Slingsby, Hit and lead criteria in drug discovery for infectious diseases of the developing world, *Nat. Rev. Drug Discov.* (2015) 1–8. doi:10.1038/nrd4683.
- [84] X. Hu, Y. Hu, M. Vogt, D. Stumpfe, MMP-Cli ff s: Systematic Identi fi cation of Activity Cli ff s on the Basis of Matched Molecular Pairs, (2012) 1–8.
- [85] D. Bajusz, A. RÁCZ, K. Héberger, Why is Tanimoto index an appropriate choice for fingerprint-based similarity calculations?, *J. Cheminform.* 7 (2015) 1–13. doi:10.1186/s13321-015-0069-3.
- [86] G. Landrum, RDKit: Open-source cheminformatics, (2014) <http://www.rdkit.org/>.
- [87] B.J. Neves, R.F. Dantas, M.R. Senger, C.C. Melo-Filho, W.C.G. Valente, A.C.M. de Almeida, J.M. Rezende-Neto, E.F.C. Lima, R. Paveley, N. Furnham, E. Muratov, L. Kametsky, A.E. Carpenter, R.C. Braga, F.P. Silva-Junior, C.H. Andrade, Discovery of New Anti-Schistosomal Hits by Integration of QSAR-Based Virtual Screening and High Content Screening., *J. Med. Chem.* 59 (2016) 7075–88.

- doi:10.1021/acs.jmedchem.5b02038.
- [88] R Development Core Team, R: A Language and Environment for Statistical Computing. R Foundation for Statistical Computing, R Foundation for Statistical Computing, Vienna, Austria, 2008.
- [89] A. Cherkasov, E.N. Muratov, D. Fourches, A. Varnek, I.I. Baskin, M. Cronin, J. Dearden, P. Gramatica, Y.C. Martin, R. Todeschini, V. Consonni, V.E. Kuz'Min, R. Cramer, R. Benigni, C. Yang, J. Rathman, L. Terfloth, J. Gasteiger, A. Richard, A. Tropsha, QSAR modeling: Where have you been? Where are you going to?, *J. Med. Chem.* 57 (2014) 4977–5010. doi:10.1021/jm4004285.
- [90] A. Tropsha, Best Practices for QSAR Model Development, Validation, and Exploitation, *Mol. Inform.* 29 (2010) 476–488. doi:10.1002/minf.201000061.
- [91] K. Falzari, Z. Zhu, D. Pan, H. Liu, P. Hongmanee, S.G. Franzblau, In Vitro and In Vivo Activities of Macrolide Derivatives against, *Society.* 49 (2005) 1447–1454. doi:10.1128/AAC.49.4.1447.
- [92] S.G. Franzblau, M.A. Degroote, S.H. Cho, K. Andries, E. Nuermberger, I.M. Orme, K. Mdluli, I. Angulo-Barturen, T. Dick, V. Dartois, A.J. Lenaerts, Comprehensive analysis of methods used for the evaluation of compounds against *Mycobacterium tuberculosis*, *Tuberculosis.* 92 (2012) 453–488. doi:10.1016/j.tube.2012.07.003.
- [93] S.H. Cho, H.S. Lee, S. Franzblau, Microplate Alamar Blue Assay (MABA) and Low Oxygen Recovery Assay (LORA) for *Mycobacterium tuberculosis*, in: T. Parish, D.M. Roberts (Eds.), *Mycobact. Protoc.*, 3^o, New York, 2015: pp. 281–291. doi:10.1007/978-1-4939-2450-9_17.
- [94] S.G. Franzblau, R.S. Witzig, J.C. McLaughlin, P. Torres, G. Madico, A. Hernandez, M.T. Degnan, M.B. Cook, V.K. Quenzer, R.M. Ferguson, R.H. Gilman, Rapid, low-

1 technology MIC determination with clinical *Mycobacterium tuberculosis* isolates by
2 using the microplate Alamar Blue assay., *J. Clin. Microbiol.* 36 (1998) 362–6.
3 [http://www.pubmedcentral.nih.gov/articlerender.fcgi?artid=104543&tool=pmcentrez&](http://www.pubmedcentral.nih.gov/articlerender.fcgi?artid=104543&tool=pmcentrez&rendertype=abstract)
4 [rendertype=abstract](http://www.pubmedcentral.nih.gov/articlerender.fcgi?artid=104543&tool=pmcentrez&rendertype=abstract) (accessed April 9, 2014).

- 5 [95] N. Andreu, A. Zelmer, T. Fletcher, P.T. Elkington, T.H. Ward, J. Ripoll, T. Parish,
6 G.J. Bancroft, U. Schaible, B.D. Robertson, S. Wiles, Optimisation of bioluminescent
7 reporters for use with mycobacteria, *PLoS One.* 5 (2010).
8 doi:10.1371/journal.pone.0010777.

Highlights

- Predictive QSAR models aided design and synthesis of chalcone derivatives anti-TB
- Ten chalcone-like derivatives exhibited high anti-TB activity and selectivity
- Compounds also showed broad spectrum against others mycobacterium strains
- Compounds' high activity against monoresistant strains implies new mode of action